INTERIM TECHNICAL REPORT
GTRI Project No. 3244

TECHNOLOGY FOR SATELLITE POWER CONVERSION

By

D. P. Campbell
M. A. Gouker
C. Summers
J. J. Gallagher

Prepared for

National Aeronautics and Space Administration
Lewis Research Center
21000 Brookpark Road
Cleveland, Ohio 44135

Under

NASA Research Grant No. NAG3-282

NASA Technical Officer: W. M. Krawczonek

October 5, 1984

GEORGIA INSTITUTE OF TECHNOLOGY
A Unit of the University System of Georgia
Atlanta, Georgia 30332

GTRI
GEORGIA TECH RESEARCH INSTITUTE

1984

Interim Technical Report
on
Technology for
Satellite Power Conversion

NASA Research Grant
No. NAG3-282
Georgia Tech Research Institute
Project No. 3244

NASA Technical Officer: W.M. Krawczonek

Prepared for

National Aeronautics and Space Administration
Lewis Research Center
21000 Brookpark Road
Cleveland, Ohio 44135

Prepared by

D.P. Campbell
M.A. Gouker
C. Summers
J.J. Gallagher

Georgia Tech Research Institute
Georgia Institute of Technology
Atlanta, Georgia 30332

October 5, 1984

Table of Contents

List of Figures

List of Figures (continued)

List of Figures (continued)

List of Tables

I. INTRODUCTION

The demonstration of the use of microwave transmitters and rectenna techniques at 2.5 GHz leads to the investigation of higher frequencies (millimeter wave and IR) as potentially useful spectral regions for power transmission. In addition, the current developments in large-aperture antennas, coupled with the projected performance of high power electron beam devices and lasers for generation and array concepts for rectification purposes, make it possible to extend present capabilities of electromagnetic energy beaming and power conversion.

The IR region from approximately 7μm - 14μm must be considered for transmission of earth's emission to satellites for power conversion to operate satellite systems. Since the satellite will be oriented toward earth for its system operation, the satellite-located rectenna arrays can always be pointed toward the radiation from earth. This IR technique would allow both orbiting and synchronous satellites to operate on the earth's emission. It will be in a position to receive radiation day and/or night. The black body radiation of earth peaks in the 8-12μm region so that it is appropriate to investigate the capabilities and development of efficient power converters in this spectral region. Several questions arise as to the performance of a satellite-borne 10μm rectenna system viewing the earth's radiation. The type of power converters, their efficiency, switching capability, optimum radiation coupling techniques and the absolute sensitivity necessary to convert the low-level earth radiation to sufficient power to drive the satellite systems are examples of operational parameters which must be determined. Calculations have shown that the earth's radiation will provide sufficient power for satellite operation [1].

In addition to the possibility of employing the earth's radiation as a power source, the use of beamed electromagnetic

radiation from man-made sources for operating satellites must be explored. With the CO_2 laser operating on several emission lines in the 9-11 μm wavelength region, the investigation of power conversion techniques in the 7-14 μm region is significant. In addition to the use of rectenna technology in this region, the potential for IR power cells for earth radiation conversion is an important aspect.

The generation of sufficient electromagnetic radiation and propagation to the receiving system does not have to occur only in the infrared. The development of high-power sources throughout the electromagnetic spectrum allows power transfer at any convenient wavelength. The restrictions imposed by the atmosphere, however, limit this potential use of the spectrum to select wavelengths for which atmospheric losses are low. Adverse weather places further restrictions on usable wavelengths shorter than a few centimeters. Despite these drawbacks, it is appropriate to consider wavelengths other than 10 μm because of the possibility of employing satellite-to-satellite power transfer or beaming of coherent electromagnetic radiation from high altitude sites.

For power-transfer applications of interest in this report, both noncoherent energy beaming, such as that from earth, and high-energy coherent beaming, as in the case of laser or electron-tube energy generation and transfer, are of interest. When employing power sources at short wavelengths (millimeter waves and shorter), it is necessary that highly efficient generators, transmitting antennas, receiving arrays and power converters be available. It is unlikely that efficiencies approaching those achieved at RF frequencies for generation and rectification will be achieved in the millimeter or infrared wavelength region, but an extremely fine-beam focusing capability at these wavelengths is possible with relatively small antenna apertures. Of particular importance to power transfer at short wavelengths is the fabrication of

antenna arrays and power converters of the proper small dimensions.

Because of the importance of power transfer to satellites, the sections of this report which follow describe several aspects of the technology.

II. PROPAGATION MEDIUM

The beaming of electromagnetic radiation in the atmosphere is limited at short wavelengths by the absorption characteristics of the atmospheric molecules. The major absorbers in the millimeter wavelength region are water vapor and oxygen, whereas carbon dioxide and ozone make significant contributions in parts of the infrared. Figure 1 shows the horizontal attenuation for the millimeter wavelength region which becomes excessively large as one approaches higher frequencies. Transmission window regions exist between the peaks of the absorption lines but become extremely small as higher frequencies are approached. Between approximately 0.7 mm and 20μm, propagation within the atmosphere is very difficult, limited by high attenuation mainly by water vapor. For vertical transmission, curves from a paper of Mizushima [2] demonstrate the transparency of the atmosphere in the frequency range below 1 THz. Figure 2 shows the transparency at ground level for four humidities (0%, 10%, 50% and 100%) [2]. For high humidity (~100%), transparency of 75% or greater for windows can occur only at 94 GHz and below. Figures 3 and 4 show the same transparency curves for altitudes of 2 km and 4 km respectively. From these curves, it is seen that, for 100% humidity, it is possible to exceed 75% transparency in the 140 GHz window at 2 km and in the 220 GHz window at 4 km altitude. Mizushima [2] assumes for these calculations that the earth's atmosphere contains 20.95% of $^{16}O_2$ at all altitudes. The strong lines that remain at 0% humidity are the oxygen lines. On the basies of the transparencies given here, it is feasible

ATMOSPHERIC ATTENUATION

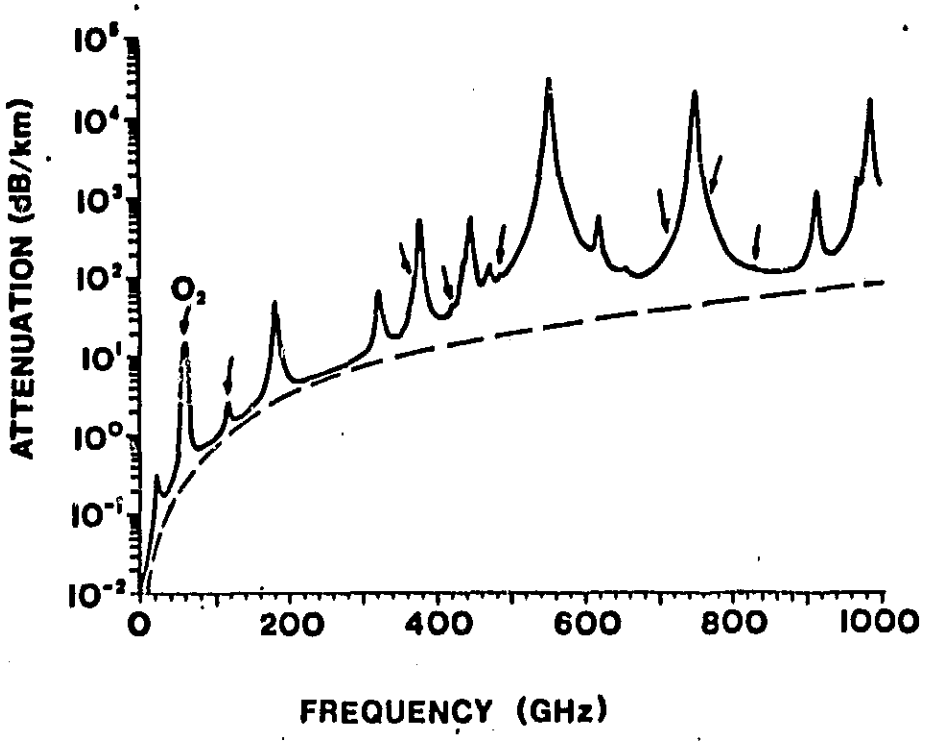

Figure 1. Atmospheric horizontal attenuation at sea level for millimeter/submillimeter wavelength region. Arrows indicate position of oxygen lines.

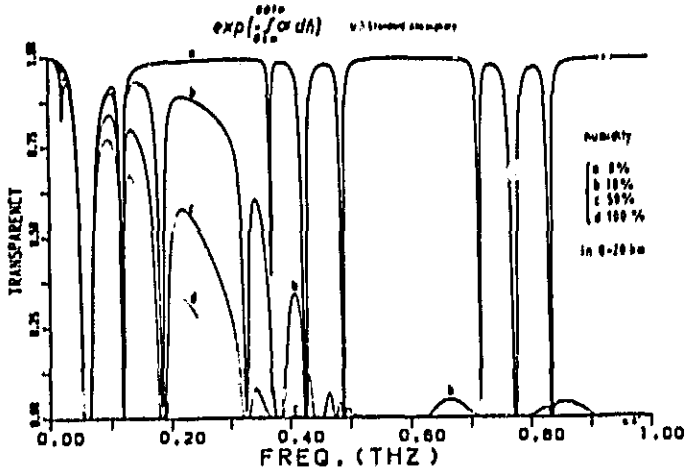

Figure 2. Transparency of the U S Standard Atmosphere at 0 km altitude in 0 to 1 THz. [2]

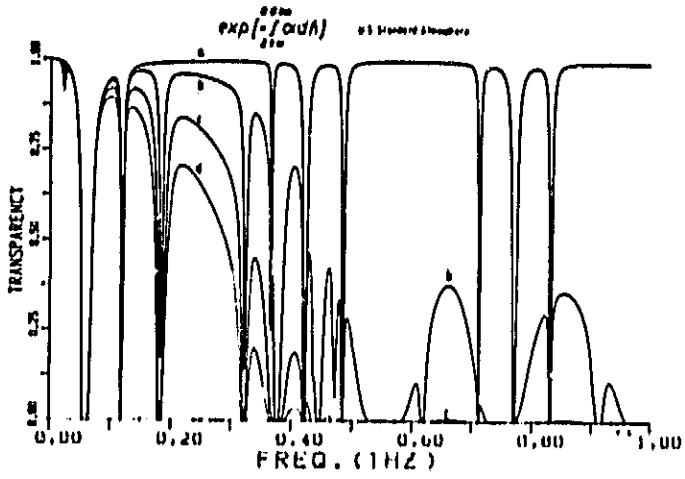

Figure 3. Transparency of the U S Standard Atmosphere at 2 km altitude in 0 to 1 THz. [2]

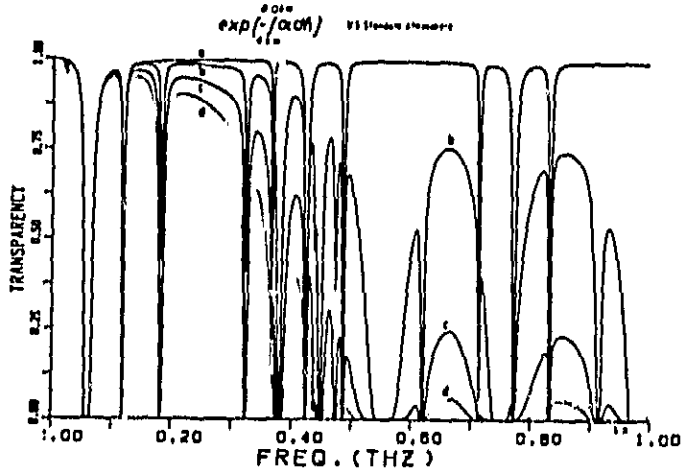

Figure 4. Transparency of the U S Standard Atmosphere at 4 km altitude in 0 to 1 THz. [2]

that power transfer to satellites can originate from sources located at high altitudes. Statistics on humidity occurrence at any proposed site must be available in order to determine applicability of a high altitude location for the transmitter.

A far more severe restriction on power transfer from an earthbound site is the occurrence of adverse weather conditions such as rain, snow and fog. Figure 5 shows a curve with rain and fog superimposed on the molecular absorption curves. It is seen that fog is a dominating factor in the infrared through visible region and that, from approximately 90-100 GHz to higher frequency into the IR, the influence of rain is approximately the same. Cloud coverage, as shown in Figure 6, can result in considerable attenuation beginning at short millimeter wavelengths and increasing with shorter wavelength. For transmission of power from aircraft-to-satellite, very low attenuation occurs in most spectral regions. Figure 7 shows the vertical transmission from an aircraft at approximately 40,000 feet altitude.

The conclusion to be drawn from this discussion is that location of a power source at high altitude might be feasible, based on the humidity and adverse weather occurrence, and that the operational millimeter region frequencies are 94 GHz and windows below this frequency from ground level, 140 GHz and 220 GHz as a function of altitude, and the IR 8-14μm region. Compared to satellite-to-satellite transfer, however, the use of earth transmitters does not appear appropriate because of potential down-time due to inclement weather conditions.

III. POWER SOURCE LOCATION

For power transfer applications for satellite systems, the optimum location of the power source will probably prove to be in a second satellite. The adverse conditions resulting from atmospheric attenuation can negate the use of earth-located sources, even though transmission from selected high-altitude

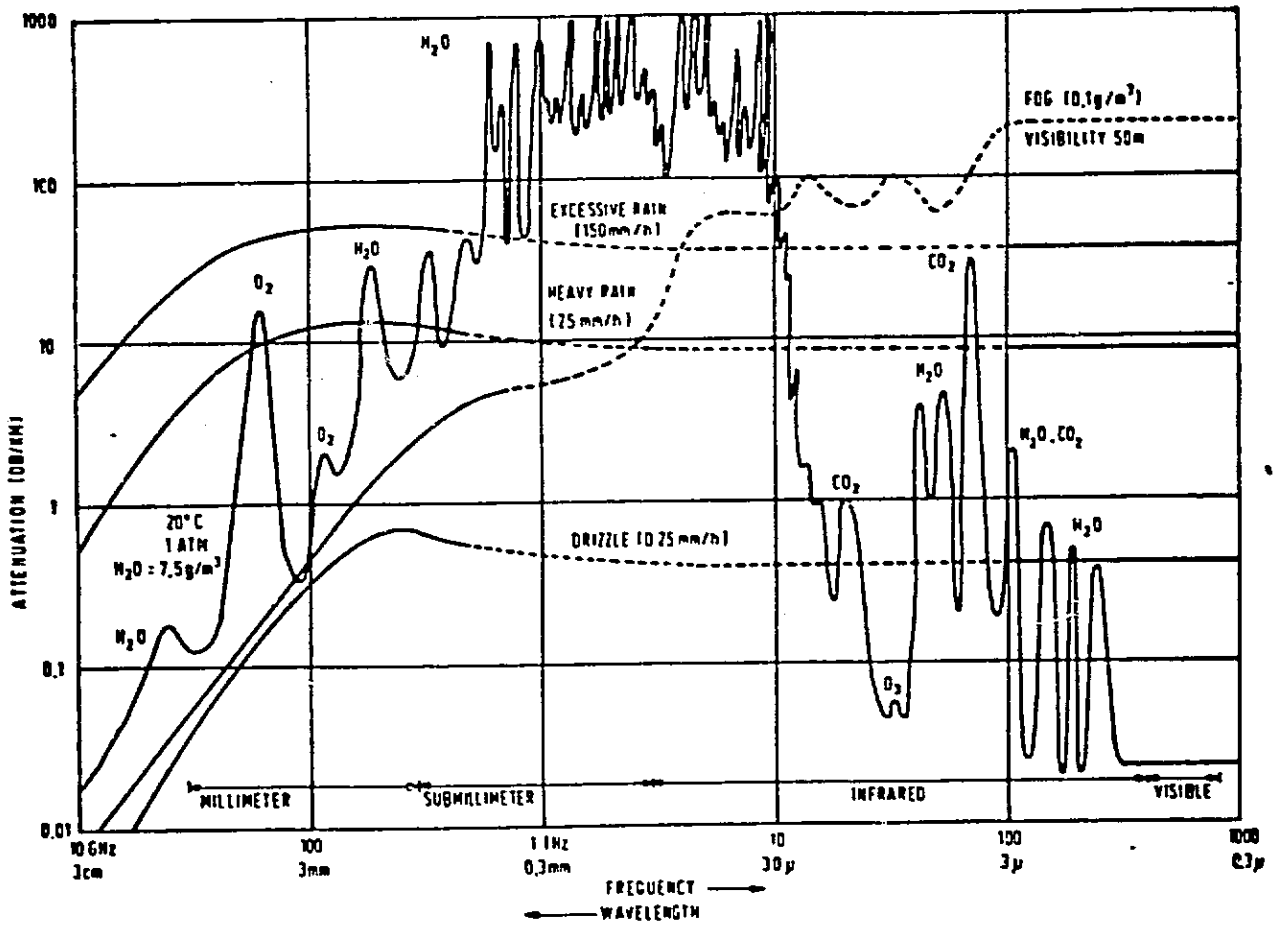

Figure 5. Attenuation by atmospheric gases, rain and fog.

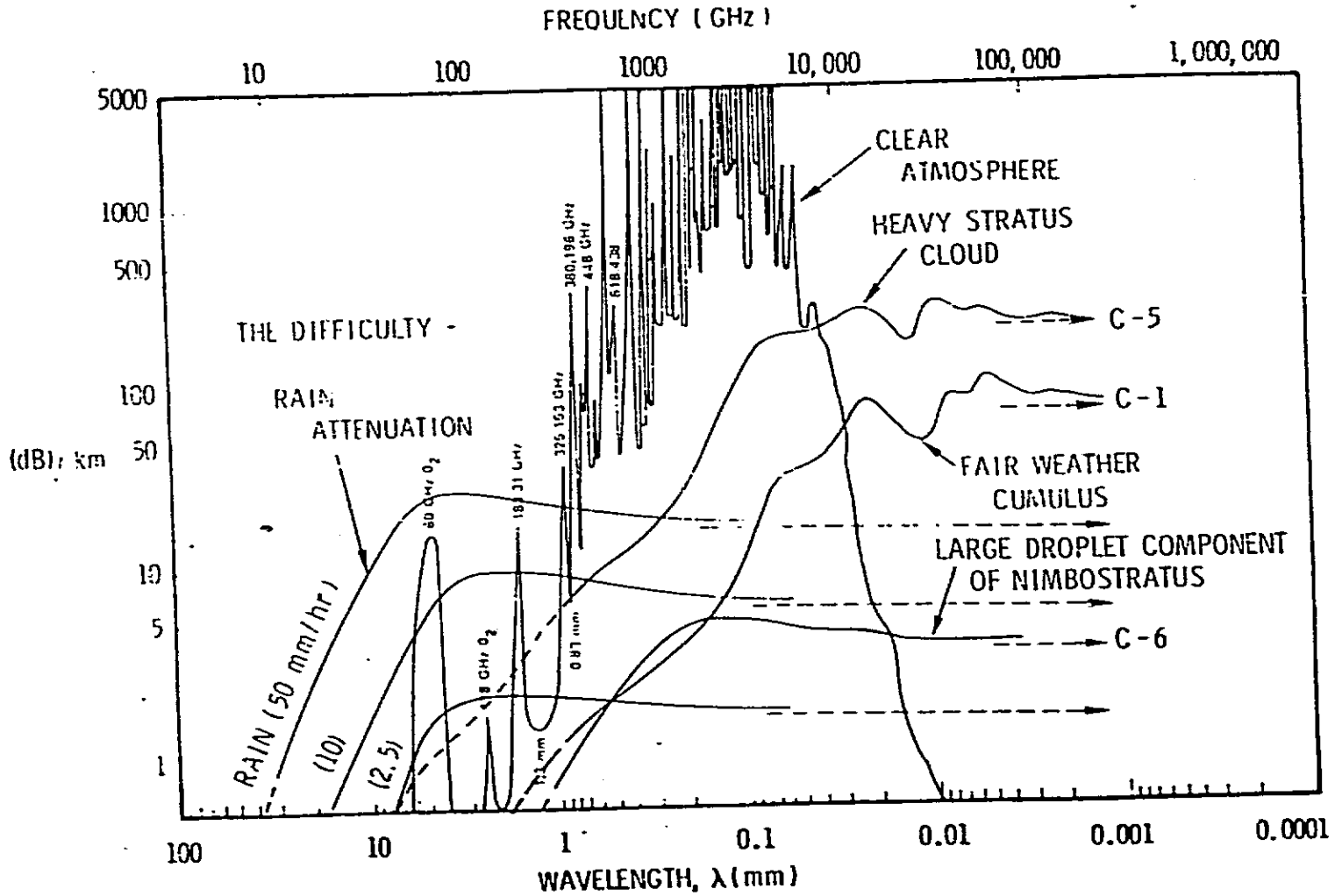

Figure 6. Summary of sea-level atmospheric attenuation.

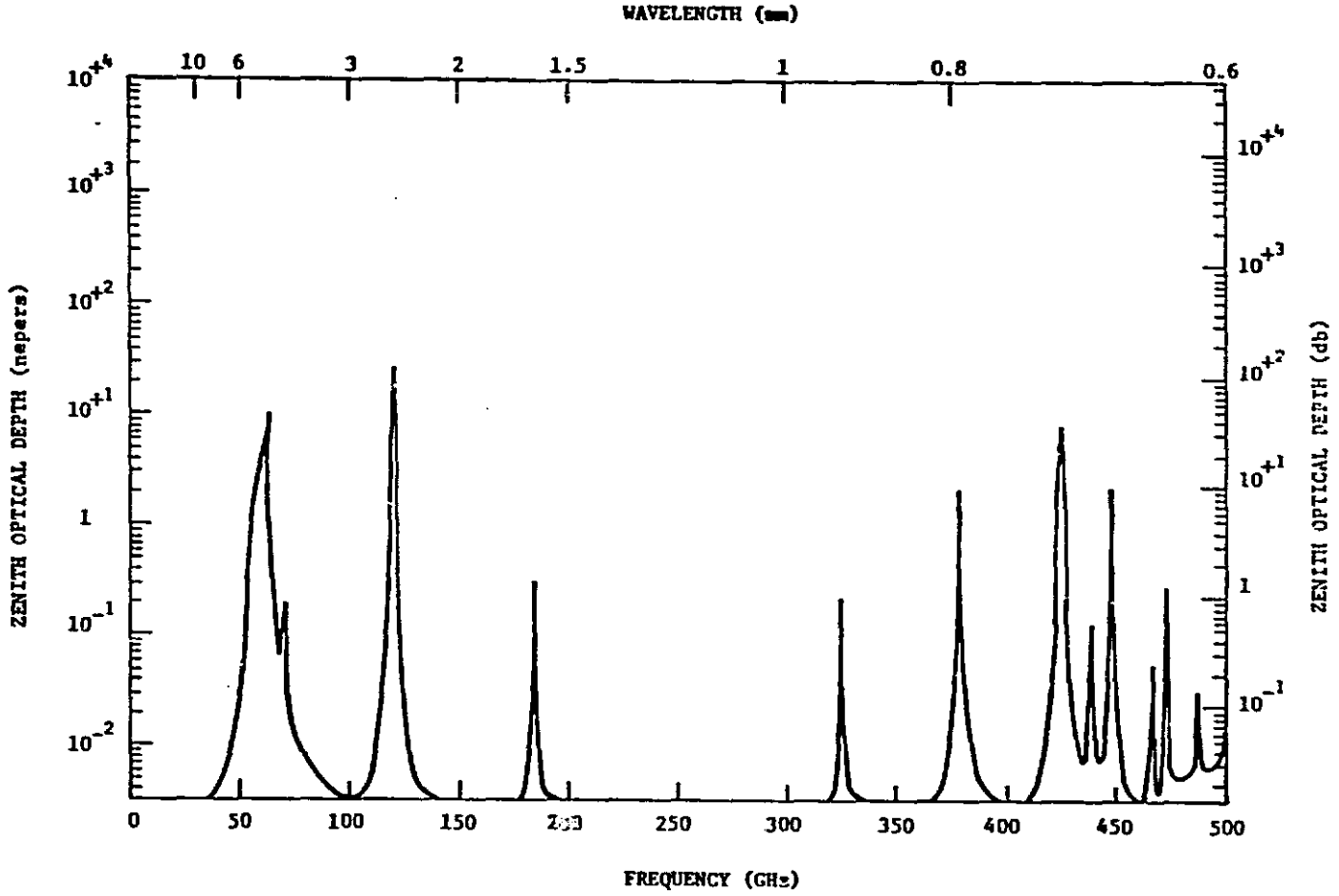

Figure 7a. Vertical Transmission from an aircraft at approximately 40,000 feet altitude. Frequency 0 - 500 GHz.

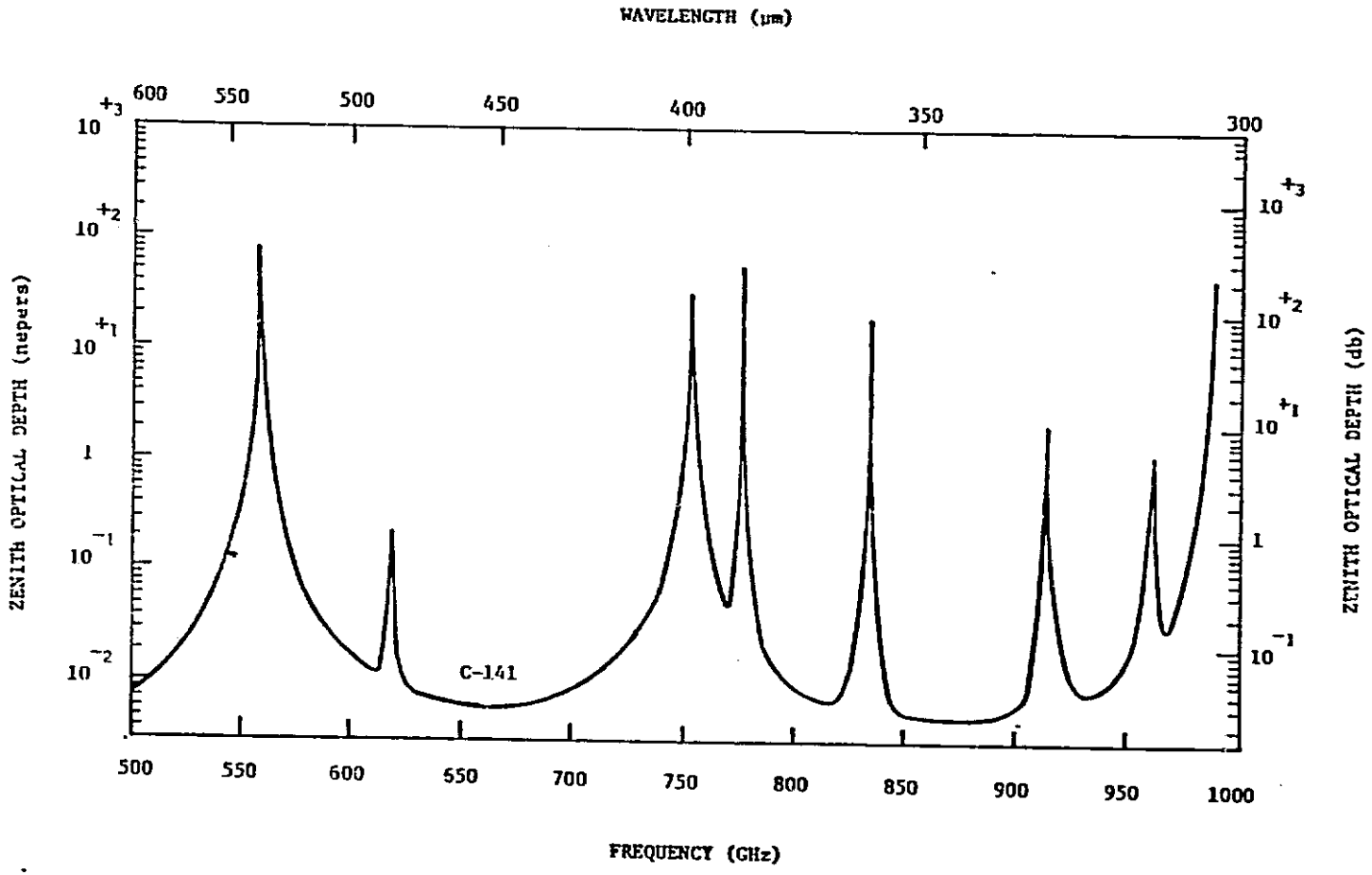

Figure 7b. Vertical transmission at 40,000 feet altitude. Frequency 500 - 1000 GHz.

locations is feasible. The transfer can be from low earth orbit (LEO) to geosynchronous (G/S), or G/S to a group of LEO satellites, or G/S to G/S. High flying RPV's, a topic of investigation at NASA/Langley, could be powered by transmitters in satellites, on earth (high altitude) or high-flying aircraft. The use of earth radiation has been shown [1] to be a potential source for satellite and RPV systems.

IV. POWER TRANSMITTERS

In the past decade, significant developments have been made in power sources. This has been the case particularly in terms of high reliability, very-high power (both peak and cw), lower unit cost, and greatly improved performance in the millimeter/submillimeter region. This effort has been supported heavily by DoD interest in millimeter wave applications, so that considerable advances in both solid state and electron tube sources have resulted throughout the millimeter wavelength region. A forthcoming publication by McMillan [3] reviews the progress of millimeter/submillimeter sources. The high frequency limit for solid state Gunn oscillators appears to be approximately 150 GHz whereas the high frequency limit for solid state IMPATT sources is probably 300 GHz. In addition, solid state sources cannot approach the performance of the electron tube devices in both power output and efficiency. The upper frequency limit of electron tube devices also far exceeds that of solid state sources. Laser devices, on the other hand, extend the potential for power transfer from the submillimeter wavelength region into the infrared.

Recent achievements in vacuum tube technology have resulted in extension of operation in frequency, power and efficiency. Extended interaction oscillators (EIO's), backward wave oscillators (BWO's), oratrons, gyrotrons and free electron lasers (FEL) have all been demonstrated to operate well above

the 200 GHz range. Of these devices, the gyrotron and FEL have power levels and efficiencies appropriate for power transfer in the millimeter through infrared regions.

A. Gyrotron

The gyrotron, however, is the most desirable for this application because of its capability to operate in the cw mode and because of its high efficiency, but because of the magnetic field requirements, it must operate with superconducting magnets or in higher harmonics of the cyclotron resonance in order to achieve high frequency operation. Until efficient cw operation for the FEL is achievable, the gyrotron will be considered the significant source for power transfer in the millimeter/submillimeter wavelength region. The FEL can, however, operate into the optical region whereas, because of the limits mentioned above, practical use of the gyrotron is probably limited to frequencies well below 500 GHz. As a result, unless very large antenna structures are used in space, beam spreading will be large and loss by spill-over of the receiving arrays will be equivalent to a low efficiency system.

Significant Characteristics

The gyrotron is a high power millimeter or microwave vacuum tube that can be operated as an oscillator or amplifier. The device employs stimulated cyclotron emission or amplification of electromagnetic waves by electrons [4,5]. The gyrotron is also known as the cyclotron resonance maser. It was initially investigated in the late 1950's, and the Russians developed it into a practical source of radiation during the 1960's and 1970's. In the 1970's, major U.S. advances were made at NRL, MIT, Yale, Varian and Hughes. It has been possible to demonstrate impressive efficiencies and power levels in the millimeter wavelength region.

The characteristics of the device are unique in that its

structure makes it most appropriate for shorter wavelengths where conventional sources have failed. This tube is an axially symmetric device with a large cathode, an open cavity structure, and an axial magnetic field. Electrons are emitted from the cathode with a component of velocity perpendicular to the magnetic field so that they are caused to spiral as they are accelerated through the magnetic field to the collector. This spiraling occurs at the cyclotron frequency of the electrons, and this is the frequency of radiation of the source. It is also possible to use the radiated harmonics of the cyclotron frequency. With this coupling between the electron beam and the radiation field, it is possible for the beam and circuit dimensions to be large compared to a wavelength. As a result, power density and related dimension problems are avoided in these sources. Very high output power and high efficiencies are possible for gyrotrons.

The gyrotron can be a single-cavity oscillator, or amplifier using several resonant cavities or traveling-wave circuits.

The gyrotron, as well as the free electron laser, can be thought of as consisting of three elements - the electron beam, an external pump field and an imposed radiation field [6]. The pump field can be any field that causes moving electrons to oscillate transversely. This is also called the "wiggler" and can consist of a periodically rippled static magnetic field.

There are several characteristics associated with the gyrotron that must be accounted for in optimizing a cyclotron resonance device. If not assessed or corrected for in a device, detrimental effects can occur. Excessive spread in the velocity of the electrons can greatly reduce bunching and the extraction of energy, particularly at shorter wavelength. Experimenters commonly use magnetron injection guns to produce electron beams for gyrotrons, as these thermionic sources can generate several amperes and electron energies as high as 100

keV. Different types of sources require electron guns designed for the particular system.

To generate millimeter wave radiation with gyrotrons, superconducting magnets are required. Thus, for operation with fundamental cyclotron radiation, one needs a 34 kilogauss magnetic field to generate radiation at 94 GHz or a field of 120 kilogauss for fundamental mode operation at 300 GHz. Many applications preclude the use of pulsed or superconducting magnets. By operating at high cyclotron resonance harmonics, one can overcome the need for superconducting magnets because the required magnetic field is reduced by a factor approximately equal to the harmonic number. Efficiency at second harmonic remains high and some designs have had efficiencies higher than at the fundamental frequency. In general, the efficiency falls sharply beyond the second harmonic.

Experimenters have used two approaches for efficiency enhancement - 1. an increase of radius of the cavity wall longitudinally, and 2. keeping the radius of cavity wall constant, vary the longitudinal external magnetic field.

To increase cavity volume and thereby avoid excessive thermal loading and competition among modes, high power millimeter wave gyrotrons will have to operate in highly "overmoded" cavities, i.e. in cavities that support many frequency modes at the same time. It has been shown [7] that one can stabilize highly overmoded cyclotron-resonance masers by adding a small prebunching cavity in front of the large energy-extraction cavity.

The characteristics which have been discussed here have been investigated by several laboratories in research toward practical fieldable radiation sources. Of interest for military applications are sources for millimeter wave advanced radar, electronic countermeasures and high frequency wideband communications systems.

Summary of Current Capabilities

Great progress has been made in United States laboratories since the mid-1970's when the major efforts in this country started. The gyrotron has, for various applications or projection of applications, taken several forms as amplifiers or oscillators. These sources have been called gyro-klystrons, gyro-TWT's, gyro-magnetrons, etc. according to the tube principle being followed. Whereas many applications and funding of gyrotrons are for the fusion programs, the source development plays a critical role in the plans of the Department of Defense and can contribute to power transfer techniques.

Very high efficiencies and power levels have been achieved in both pulsed and cw operation. Thus, in 1983, Varian [8] achieved cw power levels in excess of 200 kW at 60 GHz, the highest average power ever produced by a microwave tube in the millimeter wavelength region. Also reported are 340 kW cw in 28 GHz oscillators, 240 kW peak power at 60 GHz with a 100 millisecond pulse length and 350 kW short pulses at 35 GHz. In these cases, efficiencies as high as 50% were achieved.

A high power 95 GHz gyro-TWT amplifier has been developed [9] to produce in excess of 20 kW and is the best power amplifier in this spectral region. The device uses a Pierce-type gun and transverse momentum is imparted to the beam by means of a beam wiggler. The gain exceeds 30 dB. A conventional magnet generates the field in the gun and wiggler region and a superconducting magnet of approximately 33 kilogauss provides the cyclotron resonance field. Tests have shown the following characteristics:

Approximately 500 W pulsed power from an EIO has served as the driver to produce 20 kW output. This system has provided the maximum efficiency. In the case of a 10 W cw EIO driver, 17.5 kW output has been achieved with a small signal gain of approximately 33 dB. The measured bandwidth was greater than 2

GHz.

As indicated in summarizing the characteristics of gyrotrons, a technique for enhancing the efficiency of gyrotrons employs shaping of the magnetic field while maintaining the radius of the cavity constant. Read and Chu [10] have investigated these techniques by profiling the applied magnetic field in the cavity region with active coils and shaped steel collars. Efficiencies to 65% at power levels of 1 to 100 kW cw have been possible at 35 GHz. Field tapering enhanced efficiencies by a factor of 1.5 to 1.9. The method should be applicable to 100-150 GHz and to 220-300 GHz for second harmonic with superconducting magnets.

Temkin and his colleagues at MIT achieved power levels of over 180 kW at 140 GHz and indications are that, as applications demand, operation can successfully be achieved at higher frequencies.

The gyrotron activities currently being conducted in U.S. laboratories have resulted in remarkable advances in all areas investigated in less than a decade (actually since about 1977), and reports continue to show improvements. A forthcoming report by Dr. Robert Parker of NRL will detail the current status and state-of-the-art of gyrotrons. It will also show the enormous advances made in tube technology for the funding provided, in particular in its comparison with solid-state technology.

Trends in Technology

The technology will continue to improve operation of existing apparatus in efforts to meet requirements of both military and civilian applications. Tradeoffs will be made between oscillators and amplifiers as the appropriate sources for particular applications. Thus, a case reported [10] has resulted in the dropping of a gyro-klystron amplifier in favor of gyro-oscillators despite the fact that the amplifiers have

shown over 40 dB gain in experimental apparatus. However, efficiency problems and dilution of efforts have resulted in the change. In the work lying ahead, concentration on specific types of sources may be necessary in order to avoid spreading efforts too thin.

Among the technologies that will be developing and are already under investigation are:

1. Prospects for practical gyrotron amplifiers are encouraging. Researchers at NRL have achieved gains of 18 to 56 dB over large useful bandwidths at frequencies in the K_a-band region with a typical power of 10 kW.

2. A trend toward higher frequencies is necessary. Investigations toward replacing the cavity with open resonators are being performed to allow one to operate at submillimeter wavelengths, to select modes and to handle extremely large powers.

3. Work continues toward better waveguide couplers for beam and RF separation in high power gyrotrons.

4. Gyrotron oscillators and amplifiers require an entirely different type of electron gun. It is necessary that an ideal beam must have proper geometry not only to maximize RF interaction with selected waveguide circuit mode but for maximum efficiency. Among the factors toward which investigations must be pointed are:

the transverse velocity of electrons must exceed the longitudinal velocity by a factor of 1.5 to 2;

the spread in longitudinal velocity must be small, approximately 10-20% for oscillators and 2-5% for amplifiers.

The velocity spread from some guns has been excessive for amplifier work and has precluded the attainment of high efficiency in these devices, but these guns have been adequate for oscillators. Work has been progressing on new single-anode, MIG-type guns for gyro-TWT's.

5. Areas of importance that have been treated by Jory et

al [11] include output window heating, beam distribution in collectors and output mode purity. The mode purity requirements, so important for practical sources integrated into a system application, have been found to be typically in conflict with a conservative beam power density in the collector. The conflict must be resolved to achieve the 200 kW cw oscillator for operation at 140 GHz as discussed by Jory et al [12]. The Varian investigators are considering trade-offs with various interaction cavity modes.

6. The magnetic field requirements of gyrotrons have caused difficulties in establishing practical sources for systems applications. As indicated above, the magnetic field can be reduced by a factor of 10 if the device is operated at the 10^{th} cyclotron harmonic but high cyclotron harmonic operation requires beams with energies in excess of 100 keV, leads to difficulties in mode competition, and operates at considerable reduction in efficiency compared to fundamental harmonic operation. Destler [13] has demonstrated that putting vanes in waveguide, thereby encouraging radiation at a certain cyclotron harmonic, reduces difficulty in mode competition. While successful operation at the 12^{th} cyclotron harmonic frequency of the electron has been demonstrated, the original work of Destler does not imply feasibility of low voltage operation for high cyclotron harmonics. Lau and Barnett [14] have proposed a gyro-magnetron operating at the 12^{th} harmonic with moderately low beam voltage, much less than 100 kV. The gyro-magnetron has the features of a gyrotron and conventional magnetron that operates at low magnetic fields. Initial experiments show reduction of field requirements by a factor of six.

7. It has been recommended for wide bandwidth operation to use an effect known as the Weibel instability by which a non-relativistic tube could operate with 70% bandwidth. This effect results when one electron beam interacts with the "slow"

wave in a TWT. No such device has been assembled as yet.

8. The development of microwave/millimeter wave components to handle the power output of the gyrotron is an important aspect for the use of these devices in systems applications. It has been suggested that quasi-optical components in over-size pressurized guide be employed for millimeter wave applications.

Modal purity of the output is of concern, since gyrotrons are multimode with appreciable power fractions in non-fundamental modes. Undesired higher-order modes produce degraded antenna efficiency.

9. With gyrotrons currently producing 100-200 kW, pulsed and cw at 28 GHz, 35 GHz and 60 GHz, considerable interest exists for development of a 100 GHz, 1.0 MW cw gyrotron. Recently, Hughes has developed a 100 GHz, 0.5 MW gyrotron operating at low duty at 30 msec pulse widths [15].

B. Free Electron Lasers (FEL)

The free electron laser (FEL), first designed and successfully operated by J.M.J. Madey et al [16] in 1977. In the FEL, the electron beam is made periodic so that it is possible to have energy exchange between the electrons and a "fast" transverse electric wave propagating along a smooth conducting wall waveguide or (for very short wavelengths) a "free" electromagnetic wave propagating back and forth along an open cavity simply made of two reflecting mirrors.

When the electron beam (e.b.) is modulated with a spatially periodic magnetic field (undulator magnet (UM)), the electrons are forced to follow undulated trajectories. The electrons, affected by magnetic forces, are accelerated and emit synchrotron radiation [17]. If the e.b. is traveling together with an electromagnetic radiation, with the proper wavelength, the e.b. energy is modulated by the action of the electric field of the e.m. wave parallel to the transverse

electron velocity, generated by the UM. This modulation is transformed into bunching, resulting in coherent emission. Synchronism between electrons and field is obtained by correctly choosing, for a given wavelength, the electron velocity and magnetic field intensity and periodicity. The FEL operates with a relativistic e.b., the advantage of which provides the extension of tunability. In principle, the device can radiate at wavelengths from the far infrared to the X-ray spectral region [17].

The FEL requires high e.b. quality accelerators and special magnets. The electromagnetic field which is synchronized with the electron beam is provide by a laser or coherent millimeter/submillimeter source. Table I shows a list of FEL devices currently in operation or under construction. IR FEL utilize a single passage scheme, whereas visible FEL operate a multipassage system, actually employing a Storage Ring. Renieri [17] indicates that only two devices (Livermore and Santa Barbara) will utilize a continuous electron beam and all other sources operate with RF accelerators.

C. Carbon Dioxide Laser

Any laser which will be used for power transfer must be efficient and capable of producing high power. The carbon dioxide (CO_2) laser has these advantages. The CO_2 laser has been developed as both a pulsed and cw source, and has been one of the most used lasers available. It has been used in LIDAR systems, DIAL systems, atmospheric propagation studies and laser weapon applications. A well-designed CO_2 laser has an efficiency in the 20% range.

The class of highest power CO_2 lasers is the gas transport or force convection cooled systems. This type of laser is characterized by the rapid flow of the gas medium through the laser cavity. Within this class, the highest power system is the gasdynamic laser which is capable of cw output power

TABLE I

FEL's Under Development or Operating [17]

	λ μm	ACCELERATOR	ε MeV	I A	UM	λ_q cm
LIVERMORE	$(2\text{-}10)\cdot10^2$	Induction Linac	4	10^2	Pulsed (Tapered)	9.8
SINGLE STAGE	100-360		3-6		Permanent Magnet	3.6
S. BARBARA		Pelletron		2		
TWO STAGES	1-10		3		FEL Laser Wave	10^{-2}-10^{-1}
BELL LABS	100-400	Microtron	10-20	5	Normal Conducting Electromagnet	20
FRASCATI (ENEA)	10-30	Microtron	20	6.5	Permanent Magnet	5
UK PROJECT	2-20	Linac	30-100	10	Permanent Magnet	8
TRW (Oscillator)	10.6	Superconducting Linac	66	2.5	Permanent Magnet	3.56
LOS ALAMOS (OSCILLATOR)	9-11	Linac	20	25	Permanent Magnet	2.4
MSNW-BAC	10.6	Linac	19	100	Permanent Magnet	2.54-2.22
STANFORD (Oscillator)	3.3	Superconducting Linac	43	1.3	Superconducting Electromagnet	3.23
NOVOSIBIRSK	0.6328	Storage Ring (VEPP-III)	370		Permanent Magnet	10
ORSAY (Oscillator)	0.65	Storage Ring (ACO)	166		Permanent Magnet	7.78
FRASCAII (INEN)	0.5145	Storage Ring (Adone)	360,624		Normal Conducting Electromagnetic	11.6
BROOKHAVEN	0 25 0 45	Storage Ring (VUV Ring)	300-500		Permanent Magnet	6.5

E = e.b. energy
I = Micropulse Current
UM = Undulator Magnet
λ_q = VM Period

greater than 100 kW. However, there are significant disadvantages with the gasdynamic laser. They are large in size, consume large amounts of laser gases, and in most cases limited in operating time.

Because of these limitations the gasdynamic laser is not a viable choice for the power transfer problem unless it becomes evident that the power within this system's capabilities is necessary.

There are two other lasers in the gas transport family, namely the fast axial flow and fast transverse flow, that are likely candidates for generating the required radiation for power conversion. For power transfer applications, the laser should be capable of long-time operation and high beam quality. Further, because of potential use in satellites, aircraft or from high-altitude sites, the total system must utilize closed-cycle gas flow and must be practical in terms of size and weight. Both the fast axial flow and fast transverse flow systems have been developed for industrial metal working and are commercially available with many of the required features.

The fast axial flow laser has a small gas cross-sectional area with a high gas velocity and the gas is transported very rapidly along the axis of the laser cavity. The configuration is shown in Figure 8. The second configuration utilizes the flow of gas through a much larger cross-section in a direction perpendicular to the laser cavity. This geometry is characteristic of both the transverse flow and gasdynamic lasers.

In the case of transverse flow lasers, in which the axes of electric discharge, gas flow and laser output are all mutually orthogonal, the most attractive feature for remote energy transfer is the laser's high output power for a relatively small size. Figure 9 shows this laser geometry. Output power for commercially available lasers is typically 5-6 kW with up to 20 kW for laboratory models [19]. This is

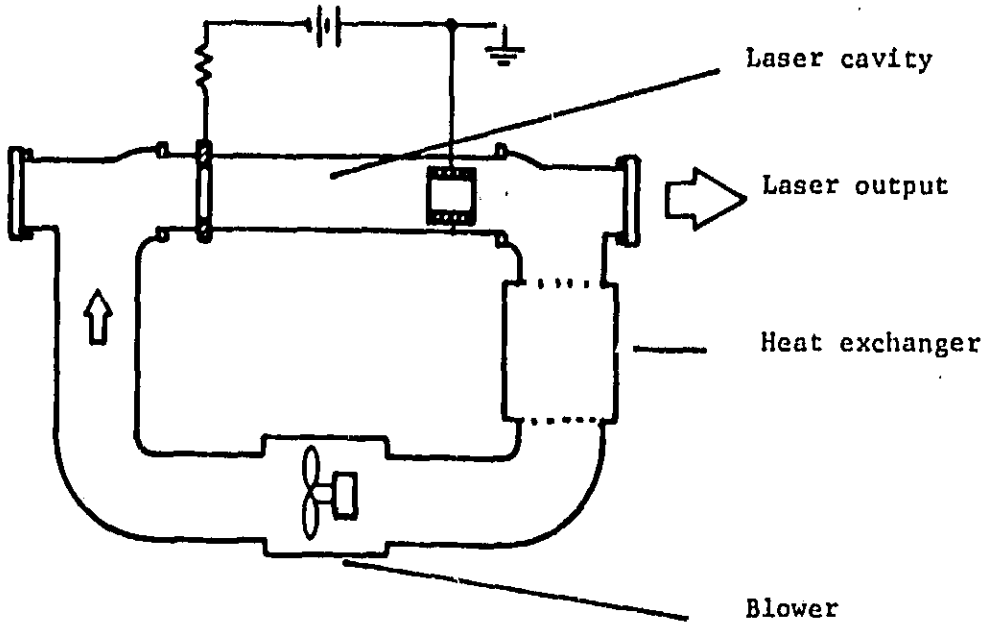

Figure 8. Block diagram of the fast axial flow laser. The gas is transported at high velocities along the axis of the output beam. The thermal energy is expelled through the heat exchanger. [18]

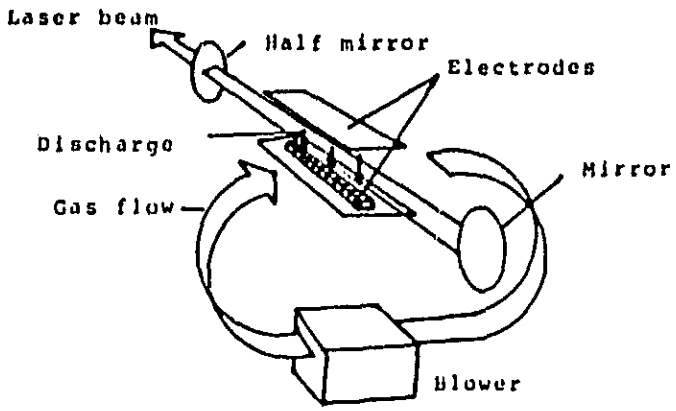

Figure 9. Block diagram of the transvers flow laser. Note that the electric discharge axis, the gas flow axis and the laser beam axis are all mutually orthogoanl [20].

possible because the gas velocity is only on the order of tens of meters per second. Compact, efficient blowers are readily available to circulate the gas perpendicular to the laser cavity, resulting in a characteristic drum shape.

The fast axial flow laser produces the most symmetric gaussian shaped beam profile of the high power CO_2 lasers. This is due primarily to the tube which defines the laser cavity as in the conventional slow axial flow lasers. In this case, the axes of the electric discharge, laser cavity and gas flow are all parallel. The tube which confines these also aids in the formation of the symmetric gaussian TEM_{oo} mode. The disadvantage of the fast axial flow system is the inherent high pressure differential across the tube and the required velocities, on the order of hundreds of meters per second, to move the gas through the tube without the onset of thermal bottlenecking. To overcome these difficulties large and fairly elaborate pumping schemes must be implemented. The end result is a total package much larger than the transverse flow laser. Further, the highest power fast axial flow system reported in the literature is 6 kW [21].

There is an inherent difference in the beam profile of the fast axial flow and the transverse flow lasers. As mentioned above, the fast axial flow laser produces a symmetric beam cross section because of the inherent radial symmetry of the tube. The symmetry and quality of the beam profile are strongly affected by gradients of refractive index in the active region. These in turn arise from temperature and pressure gradients of the laser gas [22]. In the transverse flow, these gradients occur perpendicular to the beam axis and are reflected in the beam output. The impact that this difference will have on the performance of each laser may be critical.

Other factors that should be considered in regard to the practical use of the laser are the long term stability and

system reliability and maintenance. In the gas transport lasers competition between the resonant frequencies in the cavity does not have time to develop because the gas is replaced so quickly. In this case, laser action can occur at several wavelengths independently of each other. Although there is instability for a single wavelength, the total output of the laser is constant [22]. This is an important advantage over the conventional slow flow lasers where long term stability is a problem for cavities shorter than three to four meters [23].

The long-term operation of a high power gas transport laser must still be determined. Life-time testing of these lasers has not been discussed in the open literature. For the fast axial flow laser, the weakest link in the system, at the present time, is the reliability of the blower. The current generation of high pressure, high velocity blowers is not engineered to withstand extended periods of operation. However, a new generation of blowers addressing this problem should become available shortly.

The transverse flow system appeared in the literature nearly a decade before the fast axial flow laser. One of the first systems was reported by Tiffany et. al. [24] just a few years after it became apparent that the thermal energy generated in the gas limited the output performance [25, 26].

To summarize the discussion above, the fast axial flow and transverse flow systems are the two most attractive CO_2 lasers for the power transfer problem. There are several trade offs between these two lasers when considering either for an actual application. The main advantage of the transverse flow system is the compact form and relatively small space that it requires to operate. On the other hand, the fast axial flow configuration has a radially symmetric beam profile but with a larger system size. In addition the fast axial flow system has a considerably higher overall efficiency [27]. Values as high

as 17% for the entire system efficiency have been reported by Sugawara [28].

V. RECEIVING ELEMENTS

The major consideration in developing the rectenna array is to maximize the conversion of available radiation into electrical power. Since the antennas of consideration are effective over a relatively small bandwidth, the particular design may be dependent upon the wavelength of the radiation chosen for conversion. Some of these considerations include type of antenna, substrate, type of array in which the rectennas will be place, how to maximize the antenna coupling, and what type of diode to use for rectification. In this section, considerations for developing rectenna arrays over all the frequencies of interest for satellite power conversion will be discussed. Rutledge et al [29] have written an extensive review article on integrated antennas - some of which is reported here and is distinguished by quotation marks.

The basic requirements for any antenna are acceptable patterns, impedance and efficiency. The antenna array should exhibit high gain at the expense of a narrow 3 dB width. The antenna impedance should be appropriate for the rectification element, and the efficiency must be high since there will be relatively low levels of radiation with which to work.

A. Substrate Considerations

Integrated-circuit antennas can be studied with the commonly used antenna techniques; however, there are a few significant differences from ordinary microwave antennas. The most important factor is that integrated-circuit antennas tend to radiate most of their energy into the substrate. "The complementary relations for impedance and patterns break down because they depend on duality and symmetry of a planar antenna. The presence of the dielectric makes it difficult to

apply these relations". The antenna patterns for the elementary slot and dipole on a dielectric are shown in Figure 10.

There are two major factors that cause the highly directional pattern. The first factor is inherent in the integrated circuit design. The substrate has a higher dielectric constant than air. The difference between these two dielectric constants is the primary cause of the patterns in Figure 10. "This is easy to understand for the slot, which radiates power in a dielectric proportional to $\epsilon_r^{3/2}$. Because the ground plane effectively isolates the two regions, more power goes into the dielectric, in the ratio of $\epsilon_r^{3/2}$:1. For the elementary dipole, which radiates power in a dielectric proportional to ϵ_r, it is not so obvious why its pattern is also highly oriented toward the dielectric". It is easiest to see this by thinking of the dipole as a receiving antenna. In this case, a dipole measures the parallel component of the local electric field. This local field is the field transmitted through the interface. From transmission line arguments [30] when a wave from a high-impedance material (air) is incident on a low impedance material (dielectric), the transmitted electric field is small, hence the dipole response is small [29]. "The situation is reversed when the wave is incident from the dielectric side. Now the transmitted electric field is large, and the dipole response is also large".

The other factor favoring radiation into the dielectric is the way electromagnetic waves propagate along metals at a dielectric interface. "The waves tend to propagate at a velocity that is in between the velocity of waves in the air and the velocity of waves in the dielectric. This has been verified directly from transmission lines [31] and indirectly from the resonant frequency of dipole antennas [32]. The effect is that the wave is slow as far as the air is concerned,

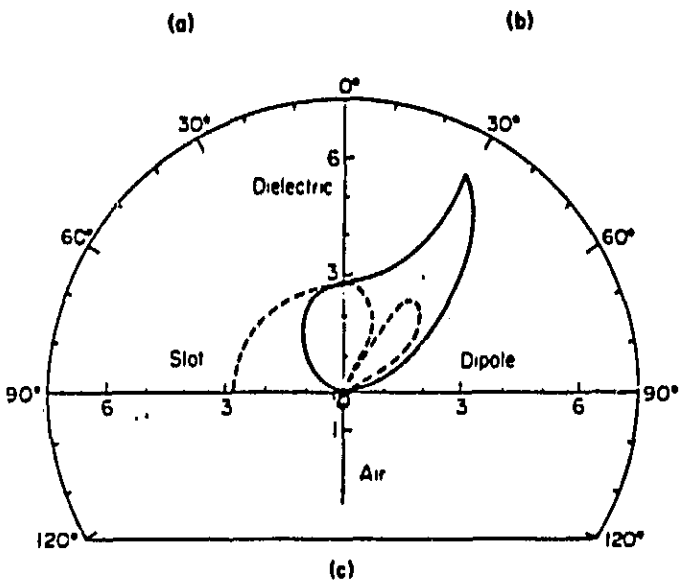

Figure 10. Contrasting radiation patterns for elementary slots and dipoles on fused quartz, $\varepsilon_r = 4$. ---, E plane; ——, H plane. The radial coordiante is gain. The slot pattern is on the left and the dipole pattern on the right. Most of the power goes into the dielectric [29].

and mainly evanescent waves are excited. On the other hand, for the dielectric the wave is fast, and the radiation is strong there. The end result is similar to that of a leaky-wave antenna [33], with the radiation primarily in the dielectric".

The performance of the antenna is also influenced by surface wave effects caused by trapped radiation undergoing total internal reflection. As shown in Figure 11, a transmitting antenna will produce trapped rays for radiation incident at angles larger than the critical angle at the second dielectric surface. The intensity of the surface waves is highly dependent upon the dielectric constant and thickness of the substrate. This effect, however, should not be significant in the rectenna arrays. For this application the distance from the source to the array will produce a highly collimated field at the antenna. Further, for maximum efficiency the antenna/array pattern should be highly directional with a 3dB width around 30-40^{o}. So there would be little antenna action if the array were rotated far enough, with respect to the incident beam, to produce surface waves.

With these considerations there are two possible substrate configurations of interest. The first, shown in Figure 12a, is the rectenna array on the appropriate dielectric with the rectennas on the opposite side from the source. In this configuration the radiation passes through the dielectric and couples to the antennas as discussed above. The second choice is to sandwich the rectenna array between two dielectrics and place a reflection plane on the rear of the second surface, as shown in Figure 12b. With antennas completely surrounded by the dielectric they behave as in free space if the wavelength of the radiation is adjusted accordingly. There are several advantages and disadvantages introduced with this configuration. First with the antenna completely immersed in the dielectric, the antenna pattern is no longer as directional

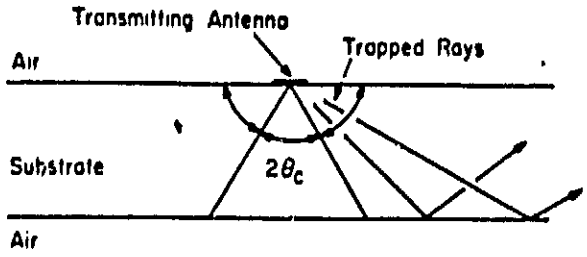

Figure 11. Transmitting antenna on a dielectric substrate showing the rays trapped as surface waves. The critical angle $\theta_c = 30^o$, appropriate for fused quartz ($\varepsilon_r = 4$) [38].

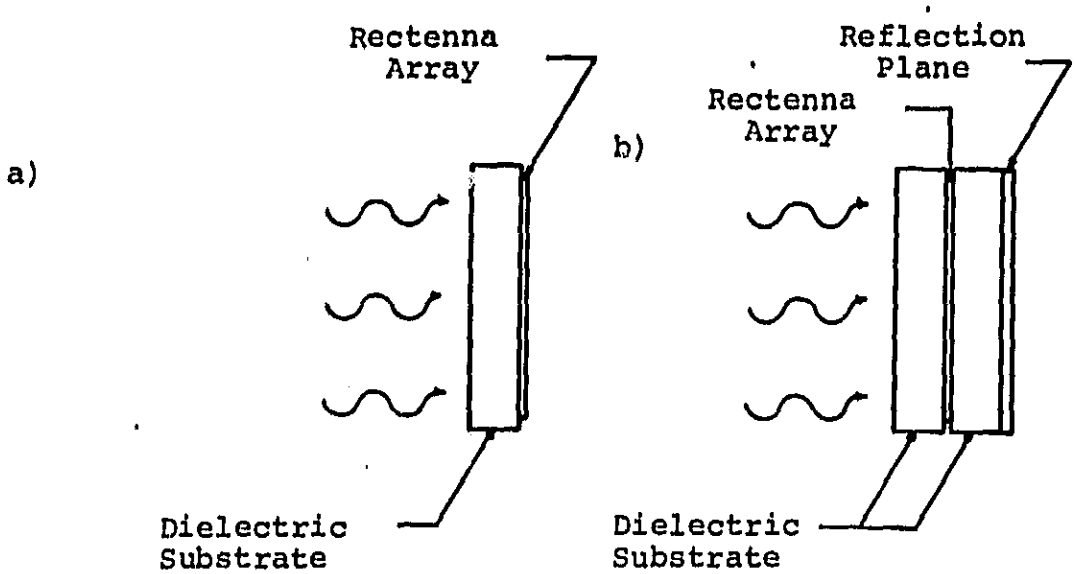

Figure 12 Two possible substrate configurations for the rectenna arrays. a) Single substrate b) Sandwiched system.

i.e. the gain is not as one sided as in 12a. A reflection plane should be introduced to promote coupling on the far side of the antenna from the source. The thickness of the substrate reflection plane would become a more critical factor in this case, since destructive interference at the array should be avoided. In addition, the second substrate would add additional weight to the overall rectenna array.

The biggest advantage of the sandwich antenna system is increased simplicity in the manufacturing process. Here the rectenna array could be made on one substrate and the accompanying circuitry on the other. Then the two halves are placed together. The major consideration in deciding between these two configurations is overall conversion efficiency.

B. Antenna Elements

The most important aspect of the rectenna array is the individual antenna element. The optimum combination of antenna pattern and efficiency along with an acceptable impedance must be chosen. There are a few possible candidates found in the literature and includes slot, simple dipole, twin dipole and bow-tie antennas.

"Little information is available for resonant slots on a dielectric. Galejs [34] calculated the radiation efficiency of a slot on the earth and concluded that most of the power went into the earth rather than into the air. Measurements by Zah [29] show patterns close to those in Figure 10, and an impedance (Figure 13) with a resonance when the length is $\lambda_m/2$, where λ_m is the wavelength calculated from the mean dielectric constant. The main disadvantage of the slot is the uniform E-plane pattern which makes it an inefficient feed antenna. However, it should be possible to correct this with a twin-slot phased array."

"Elementary dipoles on a dielectric are considerably more interesting then slots, because there is no ground plane to

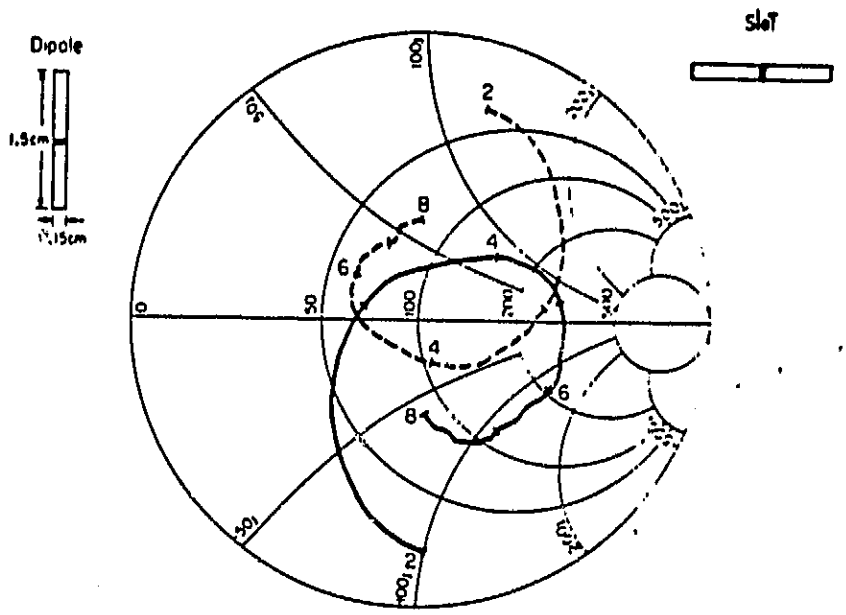

Figure 13. Measured impedance (ohms) vs frequency from 2 to 8 GHz of a resonant slot (---) and a complementary dipole (——) of the same dimensions on a dielectric with $\varepsilon_r = 4$. The frequency (in gigahertz) is given by the tick marks on the measured traces.

isolate the dielectric from the air. The exact near and far fields are quite complicated [35, 36] but usually we need to know only the fields at the antenna and far away. Brewitt-Taylor et al. [32] analyzed resonant dipoles by the method of moments, found patterns similar to those of elementary dipoles (Figure 14), and verified them experimentally. The measured impedance is plotted in Figure 13 along with the slot impedance. The resonant length is about $\lambda_m/2$".

An interesting variation of the dipole antenna was reported recently by Parrish et al. [37]. They have developed a full-wave microstrip twin-dipole array on fused quartz, see Figure 15a. This device was developed as part of an imaging array at 132 GHz. The antenna patterns, shown in Figure 15b, are very attractive with 3dB beam widths of about 40° in both planes.

The last antenna to be considered is the bow-tie antenna. This antenna combines the features of dipole radiation and transmission line radiation in an attractive way, see Figure 16. For the transmitting antenna, there is continuous radiation as a transmitted wave propagates out from the apex of the bow. "Typically the antenna can be terminated with a bow arm length of $2\lambda_d$ without affecting the pattern or the impedance. There is not yet a rigorous theory for calculating the bow-tie patterns". Figure 17a shows the measured patterns for a 10 GHz model of a bow-tie antenna [38]. Note that most of the radiation is directed into the substrate. The input impedance is frequency independent and is shown in Figure 17b.

There are several attractive features in the bow-tie configuration. They are broad band, and have been demonstrated at wavelengths as short as 119 μm [39]. They can be packed close together allowing higher system efficiencies.

The elementary dipole, twin dipole and bow-tie antennas seem to be the most promising configurations for the rectenna array. The major difference between the dipole and bow-tie antenna is the bandwidth. The dipole configuration shows more

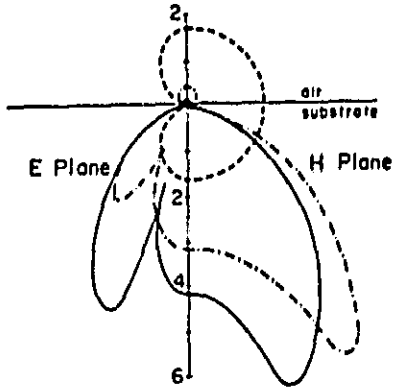

Figure 14. Calculated gain of a resonant dipole antenna on a dielectric substrate for ε_r = 1 (---), 4 (-·-), and 12 (——). The scale is linear in power [32].

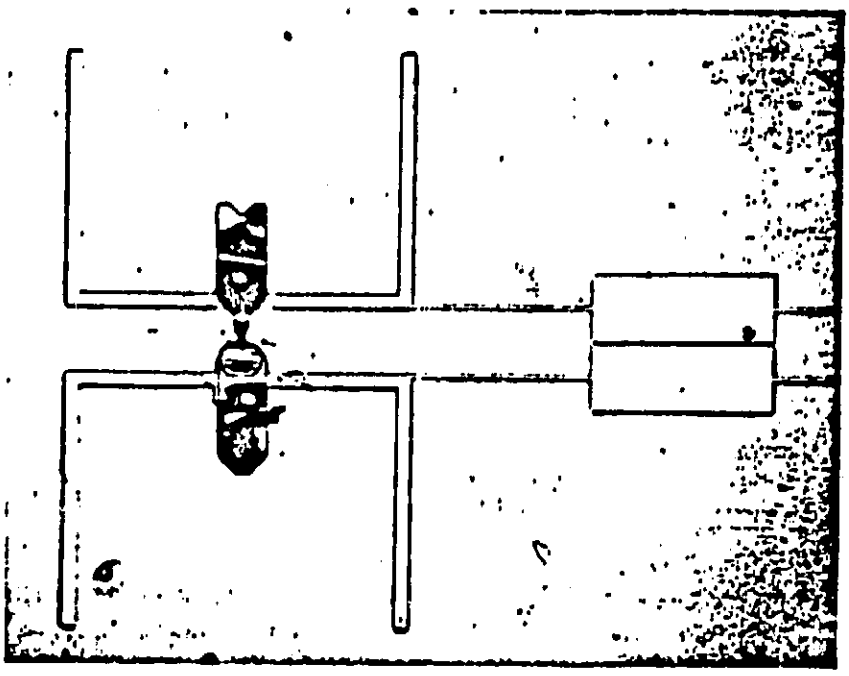

Figure 15a. Twin dipole array at 132 GHz [37].

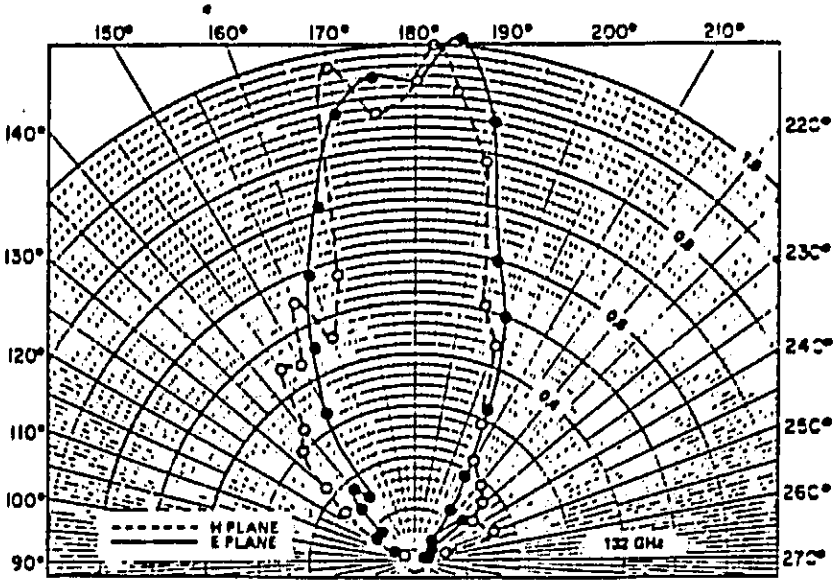

Figure 15b. Measured patterns of twin dipole array in Figure 15a [37].

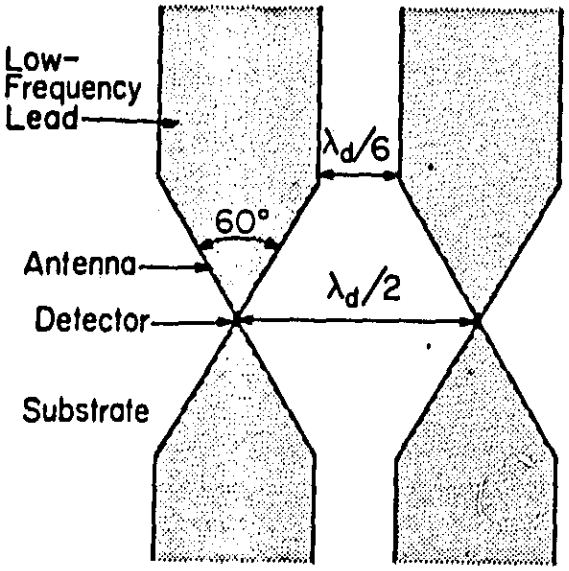

Figure 16. Bow-tie antenna array design used to test the impedance measurement technique.[38]

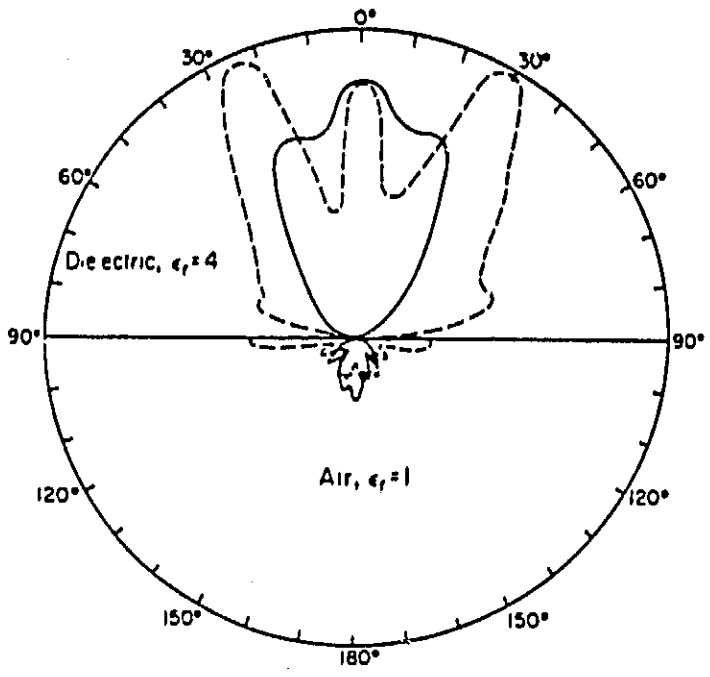

Figure 17a. Measured bow-tie antenna pattern for a 10 GHz model with $\varepsilon_r = 4$: ---, E plane; ——, H plane [38].

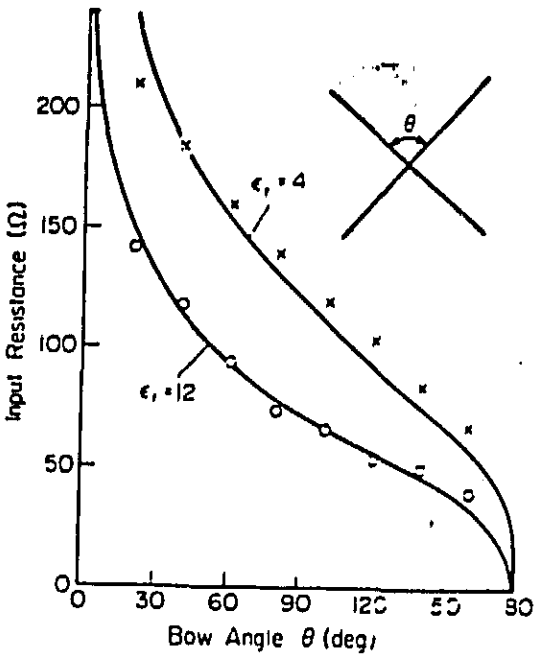

Figure 17 b. Frequency-independent resistance of long bow ties calculated from quasi-static theory: o, x corresponding measured values.[38]

resonant wavelength behavior than the bow-tie antenna. This suggests that a bow-tie may be preferable for noncoherent sources such as the earth while the dipole may be better suited to receive beamed radiation from a coherent source.

We have experience with fabrication of the elementary dipole antenna. Arrays of antennas suitable for 1.3mm wavelength radiation have been successfully fabricated and antenna action has been observed [40]. These antennas are etched from thin metal films deposited on fused silica substrates. Bismuth bolometers are used to observe the antenna action. Fabrication of the twin dipole array or bow-tie configurations should not be significantly more difficult than the techniques used for the elementary dipole antenna.

To make the rectenna array suitable for radiation of arbitrary wavelength, the physical size of the antenna element must be adjusted to optimize the coupling of the radiation. This does not seem to be a major obstacle for the frequencies of interest in power conversion. Antennas for radiation at 10.6 microns will be difficult to fabricate since the micro fabrication techniques at these dimensions will require state of the art technologies. The lower frequency limit is determined by how large an area of thin metal film can be deposited. Models of the submillimeter antennas are routinely made for 10 GHz frequencies.

C. Array Patterns

After the antenna element and suitable diode have been chosen, the rectennas will need to be placed in an array. There are two factors that need to be considered. The first is to determine the antenna pattern which optimizes radiation coupling. The second consideration is how to connect the diodes, in series, parallel or some combination of these, to produce the desired current and voltage.

Placing the rectennas into an array may have two effects

on the performance of the individual elements. First, the array factor will modify the antenna pattern of the rectennas. This could be beneficial since an even more directional total antenna pattern can be achieved. Second, if the rectennas are placed too close together, the local fields of the individual elements can overlap and modify the rectification process either for the better or for the worse.

This last consideration may be a factor in determining how the diode elements should be connected electrically. Preliminary results of elementary dipole antennas with bismuth bolometers show that it is more favorable to connect the individual elements in parallel [40]. However, this is for the passive bolometers and not the rectifying diodes so no conclusive statement can be made. Further, some combination of "parallel blocks" connected in series may have to be implemented to achieve the desired voltage and current. Such a configuration is shown in Figure 18. In this design the problem of electrical connections is solved by thin film conductors as in the printed circuit board technology.

D. Conclusions

The rectenna array is composed of four basic components: the individual antenna elements, the rectifying diodes, the substrate and the array pattern. The whole system can be scaled roughly up or down depending upon the frequency of the radiation chosen for conversion. If the source is broadband the bow-tie antenna may be the most suitable choice for the antenna elements. Conversely, the elementary dipole or twin dipole array may be more favorable for receiving radiation from coherent sources, such as gyrotrons and lasers. The rectifying diode must be fast enough to respond to the frequencies of the incoming radiation and must have the proper impedance for the desired "matched" condition with the antenna element. Finally, a suitable array pattern and substrate configuration will have

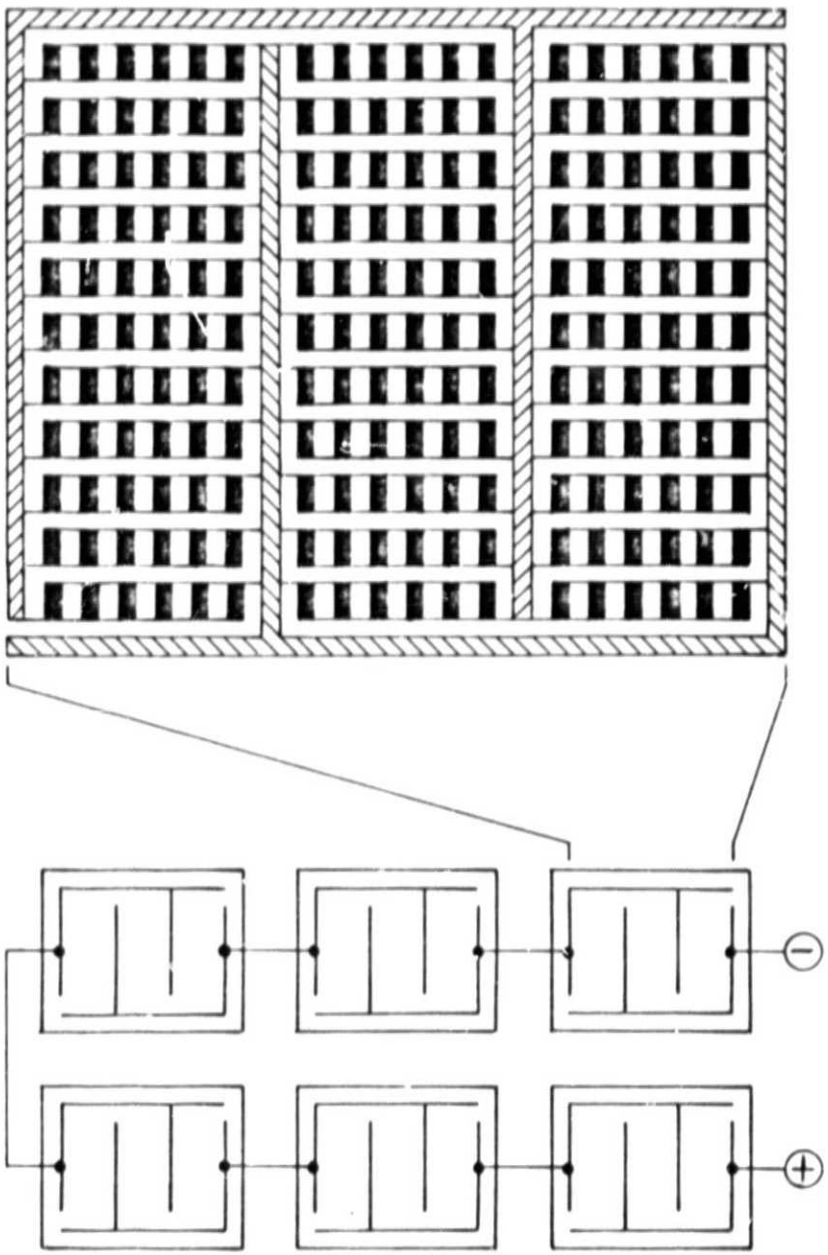

Figure 18. a) A parallel block of rectenna elements (dark rectangles). All of the diodes for the antennas in this block are connected in parallel. b) The parallel blocks are connected in series (only the major conducting paths are shown).

to be developed to maximize the coupling with the incoming radiation and provide the desired current and voltage to the satellite.

VI. POWER CONVERTERS

Metal-Oxide Metal Diodes

The two principal factors affecting the efficiency of a rectenna system are the power collection from a high-frequency source and its rectification into d.c. power. In the millimeter region, both of these mechanisms can be separated and optimized independently by the correct choice of antenna design and selection of commercially available high-speed diodes. However, the extension of this concept to higher frequencies, corresponding to 10.6 μm radiation, requires very small (micron sized) antennas and sub-micron sized rectifiers, making necessary an integrated structure [1]. The issues of the antenna design have been explained previously. In this section, the factors affecting the performance of the rectifier are discussed. Despite the progress made in the development of semiconductor devices, and the recent interest in high-speed devices, the response times of junction-type diodes are still well below the 10^{-13} - 10^{-14}s range required for this application [41]. Several new concepts promise to change this situation in the future, but at present the metal-insulator-metal device offers the only effective choice.

For efficient power output the response time of the rectifier must equal or exceed the reciprocal of the frequency of the incident radiation, and its impedance must match the antenna to optimize the power transfer between the two devices. Typically, the response time is limited by either the transit time of carriers between the two electrodes of the device, or the RC-product. Both factors are determined by the device geometry i.e. its thickness and area, and the energy band

diagram of the device which determines its current-voltage properties. The I-V characteristics also determine the rectification properties of the diode and the power density that can be conducted through the device.

As shown in Figure 19, the metal-insulator-metal (MIM) tunnel diode is a very thin film device in which electrons from one metal layer can tunnel through the insulator film and be collected by the second metal layer. The transit time of electrons across the insulator is determined by the velocity of the electron wave-packet in the insulator and the thickness of the film. Assuming a typical value of 10^7 cm/s for the electron drift velocity, insulator thicknesses of 10 and 100A are calculated for transit times of 10^{-14} and 10^{-13}s, respectively. Thus very thin structures are required for power conversion at wavelengths between 10 and 100 μm. The thickness of the insulator also limits many other properties of the diode, particularly its capacitance and load factor. The diode capacitance, C, for the thinnest structure is thus

$$C = \frac{\varepsilon A}{10 \times 10^{-8}} = 2.2 \times 10^{-6} \text{ F/cm}^2$$

where it is assumed that the dielectric constant, ϵ, of the oxide equals 2.5.

An estimate of the impedance of the device can be obtained from its electrical properties. Extensive calculations of the current-voltage characteristics of ideal MIM structures have been performed by Simmons [42] who shows that they are very strongly dependent on the oxide thickness, the built-in potentials, and the applied voltage. As shown by Figures 20 and 21, the resistance-area product of the devices increases very rapidly with oxide thickness, and near zero bias conditions increases orders of magnitude, from 10^2 to $10^{12}\ \Omega$-cm^2 as the oxide thickness is doubled from 20 to 40 Å. For

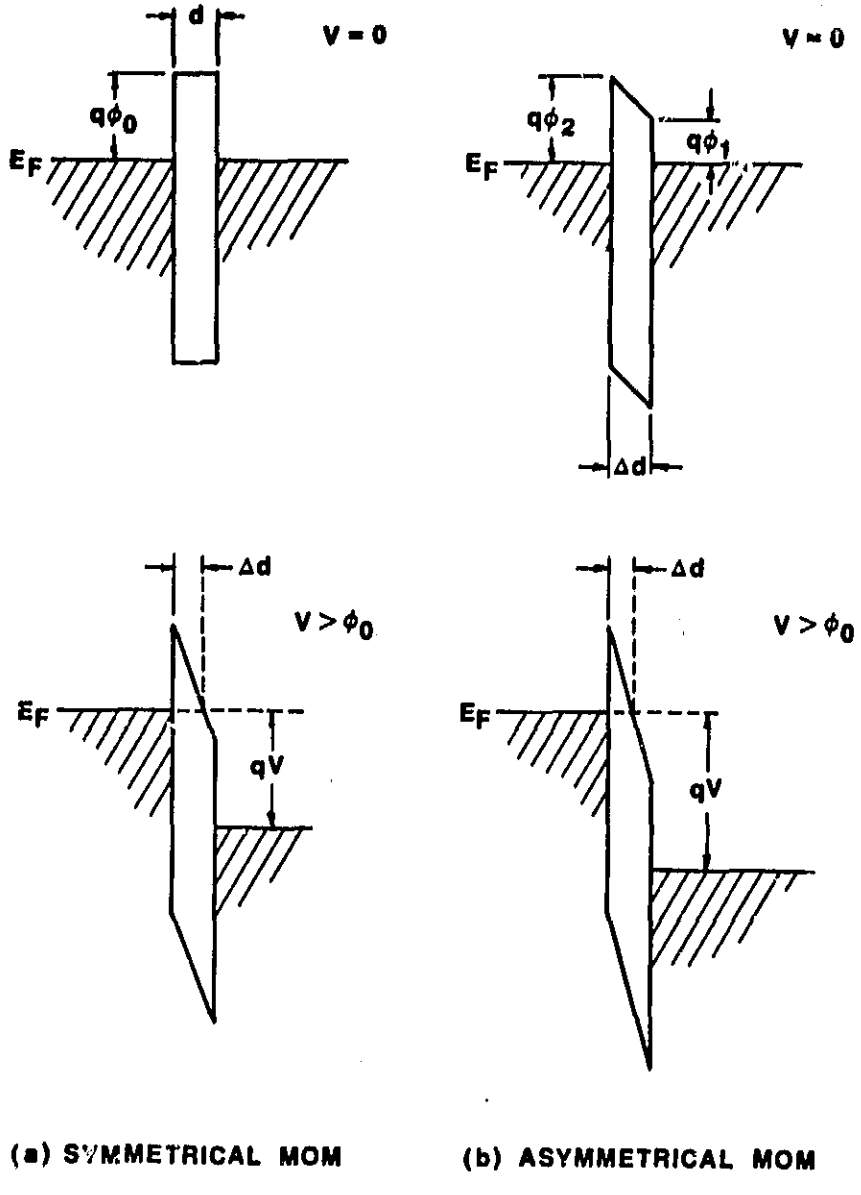

Figure 19. Possible MOM Device Structures.

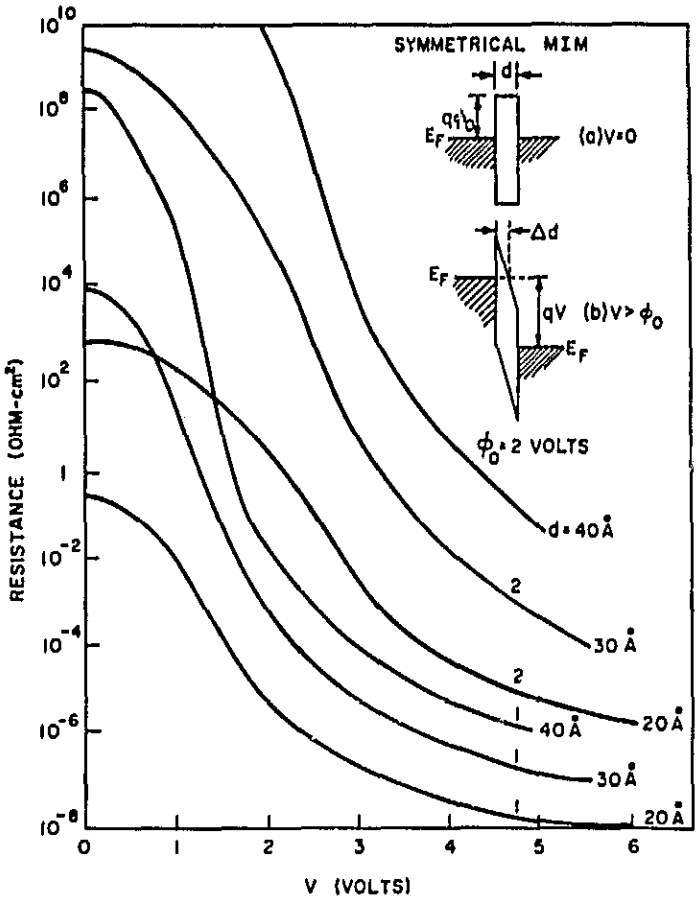

Figure 20. Tunnel resistance of a symmetrical MIM structure. The insert shows band diagrams at V = 0 (zero bias) and V > ϕ_o. (After Simmons)

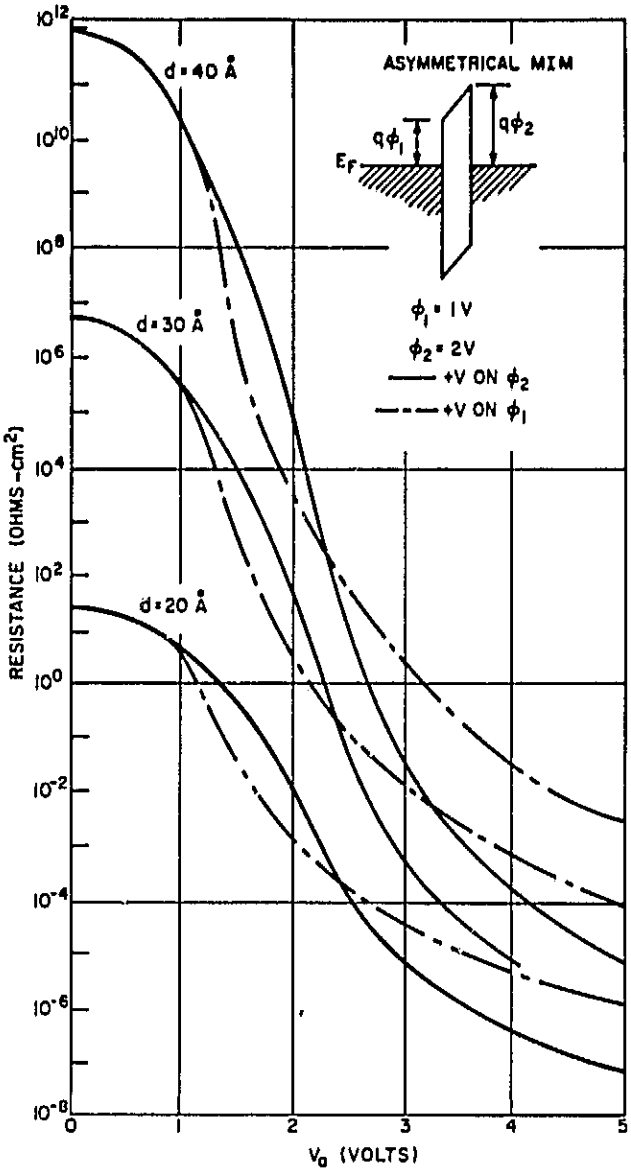

Figure 21. Tunnel resistance as a function of applied voltage for an asymmetrical MIM structure. The insert shows the band diagram at zero bias. (After Simmons.)

bias voltages greater than the built-in potential, the resistance decreases very rapidly; again the changes are by many orders of magnitude and are sufficient for the device to become highly conductive in the direction of the applied voltage. Using this information, a calculation of the RC-product shows that in fact the response time of an actual MOM structure is very slow. However, because these devices are connected in parallel with the antenna, it can be shown from the equivalent circuit of the structure, that it is the radiation resistance, R_r, of the antenna, which determines the total resistance of the rectenna. For a T-type antenna, R_r = 75 ohm, and the RC-product equals $1.65 \times 10^{-4}A$ where A is the area of the diode. Thus to obtain RC-products in the 10^{-14} - 10^{-13} sec. range, A must be equal or less than 10^{-10} cm^2. This condition limits the size of the MOM device to approximately a 0.1 μm square. Ignoring for the moment the fabrication details of these devices, it is first necessary to determine if this element size can accommodate the power transferred from the antenna to the MOM structure. To first order, the power handling capabilities can be deduced by equating the power density in the MOM device to the power density received by the antenna. For a 10 Å thick, 0.1 μm square MOM device, capable of handling 10^4 A/cm^2 at 1 volt, (Figure 19), the power load is estimated to be 10^{-6}W. The radiation power density emitted by the earth is approximately 200 W/m^2 at a distance of 100 miles above the earth's surface. For a T-type antenna whose collection area is $\sim\Pi(\lambda/2)^2$, where λ is the wavelength of the incident wavelength radiation, the antenna collection area is = 8.8×10^{-11} cm^2 for 10.6 μm radiation and it will receive 1.8×10^{-8} W from the earth. This value is more than an order of magnitude below the power density that can be conducted through a 0.1 μm square MIM device and confirms that these devices are suitable for this application. In fact the result suggests that some type of concentrator scheme could be used

to focus radiation onto the rectenna elements to achieve higher power densities. However, to achieve a concentration factor of 1000, which is presently targeted for solar cells, will require a small array of diodes attached to each antenna. For example, with a 100 diode MIM array attached to each antenna, power levels approaching 0.1 mW could be extracted from each rectenna element.

The last factor to consider is the rectification properties of these structures. These are determined by the I-V characteristics, a typical example of which for a MOM structure is shown in Figure 22. If V_1 and V_2 are the turning points in the I-V curves, then for practical applications it is required that the forward bias turning point, $V_1 \approx 1$ volt and the reverse bias turning point V_2, be significantly greater than V_1. If $V_2 \approx V_1$, then rectification will occur for both current directions resulting in a cancellation of the d.c. output. As shown by Figure 19 the R-V curve calculated by Simmons for forward and reverse bias conditions implies that the magnitude of V_1 and V_2 are approximately equal and thus this structure will not be an efficient rectifier. To obtain large V_2/V_1 ratios will therefore require very asymmetrical diode structures with the potential difference between the two metals exceeding several volts. Detailed calculations to estimate the characteristics of these structures and the effect of highly asymmetrical structures on the carrier transit times are therefore required to assess their full potential for this application.

In conclusion the above discussion shows that MOM devices should be suitable for the rectenna concept, but that further studies of these properties are required. Also for this application the devices must be very small; approximately 10 Å thick and 0.1 μm square.

Historically, these devices have been very difficult to produce, but recently Heiblum et al.[43] have developed a

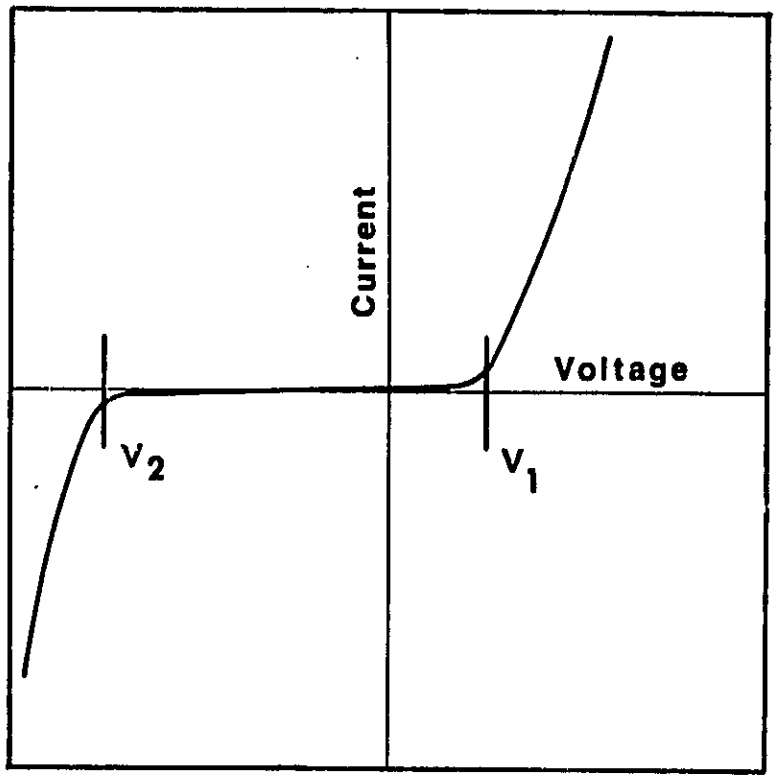

Figure 22 . Current-voltage relationship for MOM device.

structure which is stable and reproducible. A schematic of this structure which was fabricated from Ni and its oxide is shown in Figure 23. As shown, the overlap between a 1 μm thick Ni layer and the oxidized edge of another Ni layer, 5 μm wide and 100 A thick, is used to make MOM structures with areas of 10^{-10} cm^{-2}. The thickness of the oxide film is approximately 10 A and the device has been tested and shown to have frequency independent I-V characteristics up to the near infrared region. However, despite the success achieved by Heiblum, we believe that this approach will be extremely difficult to apply to large arrays. For the fastest devices, the required insulator film thicknesses correspond to three or four atomic layers of oxide and thus a variation of one atomic layer will have a large effect on device performance. To achieve atomic layer precision in the growth of a non-crystalline device constructed from dissimilar metals will be extremely difficult especially for array structures. Thus at present, we believe that the specifications required for the MOM diode exceed the currently available technology and for large arrays are not practicable. However, because the antenna and device dimensions scale linearly with wavelength, it should be possible to investigate this concept at longer wavelengths. Thus the proposed work at 119 μm and 1 mm will provide a true test of the concept as well as having a significant impact on far-infrared and millimeter imaging techniques.

Because of these problems we have considered other possible fabrication techniques and concepts. The rapid advances occurring in the fabrication of semiconductor integrated circuits using the AlGaAs system make it attractive to consider if this technology can be applied to this problem. A major disadvantage of using these materials is that the higher refractive index of the substrate requires that the antenna geometries be significantly smaller. This disadvantage is more than offset by the greater flexibility of the new

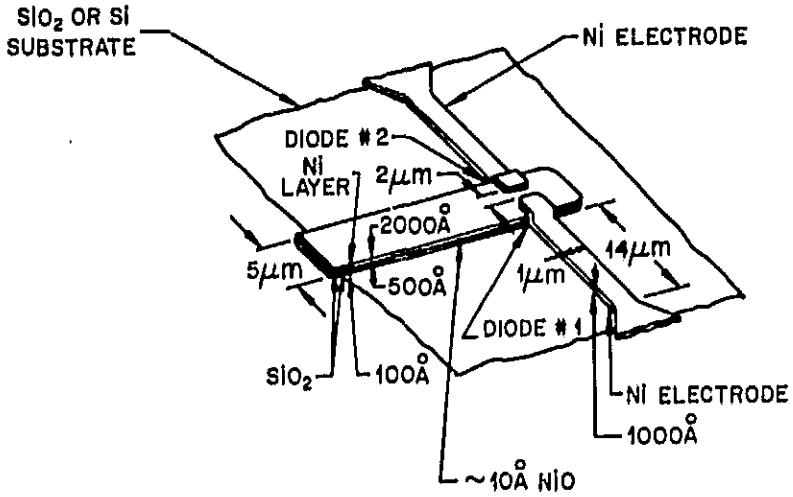

Figure 23 Schematic diagram of Edge-MOM diode. (After Heiblum et al.)

semiconductor growth technologies, such as MBE and MOCVD, to grow very thin semiconductor and metal films. For example, MBE enables GaAs layers of one or two atomic layers thick to be deposited in a reproducible way. Also ultra-thin crystalline Al films have been deposited on GaAs and at present work is directed toward obtaining the growth of thin crystalline GaAs layers on a crystalline Al surface. If this is successful it will become possible to grow a wide variety of devices. It should be noted that this is already possible to some extent by the use of heavily doped n- and p-type GaAs layers which have metallic-like properties. Thus one can envision fabricating the antenna and device arrays together in a series of growth/processing procedures. A possible structure would consist of an antenna fabricated from heavily doped n+ GaAs (or Al), with the diode consisting of a thin layer of undoped GaAs sandwiched between the antenna arms at the base of the structure. This structure would be fabricated by first depositing a 1-2 μm thick layer of heavily doped GaAs on to a semi-insulating GaAs substrate, and then using photolithography and etching procedures to remove all of the GaAs layer apart from an array of individual elements shaped like one side of the antenna. The other side of the antenna would then be defined by a SiO_2 or Si_3N_4 mask, which is required to resist the high temperature experienced during the second growth step. This growth procedure will consist of the deposition of a thin 10-100 Å epitaxial layer of undoped GaAs, followed by the deposition of a 1-2 μm thick layer of heavily doped n-type GaAs. Thus the thin undoped GaAs layer will then be sandwiched between two heavily doped layers of GaAs thereby forming a small area asymmetrically doped n++- n - n+ device. The I-V characteristics of this semiconductor-insulator-semiconductor device are similar to those of a MOM device and can be varied by changing the geometry of the device or by growing structures in series. Although this approach is still very difficult, it

offers greater control and flexibility in obtaining devices with the required characteristics. We therefore recommend that the potential of this technology also be theoretically and experimentally investigated, along with the properties of more conventional MOM devices.

VII. FABRICATION OF ANTENNAS

The construction of the antennas is dictated by the shape of the antenna, the wavelength of the incoming radiation, type of detecting or rectifying device, the substrate and whether the antenna is placed on or in the substrate. For the half-wave dipole antennas, which are being studied at Georgia Tech, Table II lists the antenna's dimensions with respect to wavelength and substrate.

The first antennas were constructed to receive 1-mm radiation. They were composed of gold over chromium, both RF sputtered onto fused silica discs. The detecting devices were DC sputtered bismuth bolometers. After testing the antenna's characteristics, the bolometer is to be replaced by the diode needed for rectification and power conversion. Then both the antenna and diode are to be reduced to receive 119 μm and finally 10.6 μm radiation.

After initial difficulties were worked out, construction of working bolometers and antennas become routine for 1 mm. When the 1 mm wavelength source (300 GHz carcinotron) power supply failed, the construction of antennas to couple with a 1.31 mm source (229 GHz) proved straightforward.

Standard photolithographic techniques work well for antennas in the 500 μm range and initial indications look good for the construction of antennas one-tenth that size. We will be incapable of extending these techniques to the small size antennas not due to photoresist limits but due to resolution of our mask making. The fly's eye camera used has a resolution limit of a couple of microns. This puts an in-house limit on

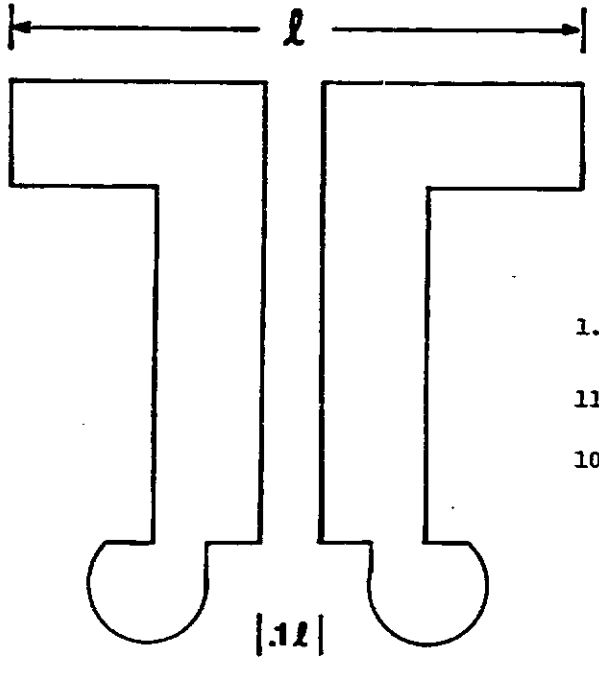

λ	ν	air (ε = 1)	on SiO_2* (ε = 3.83)	in SiO_2	on GaAs* (ε = 12.5)	in GaAs
1.31 mm	229 GHz	655 (66)	537 (54)	334 (33)	364 (36)	184 (18)
119 μm	2.52 THz	58.5 (5.9)	48.0 (4.8)	30.4 (3.0)	32.6 (3.3)	16.5 (1.7)
10.6 μm	28.3 THz	5.3 (.5)	4.3 (.4)	2.7 (.3)	3.0 (.3)	1.5 (.15)

*reduction factor for antennas on substrate extrapolated from K. Mizuno, Y. Daiku and S. Ono, IEEE Trans. Microwave Theory Tech., MTT-25, 470 (1977).

Table II. Antenna Length ℓ & (gap size .1ℓ) in μm on and in various substrates.

an antenna sized for radiation in the 25-30 μm range and then only on a low refractive index material such as fused silica. However, outside services are available which can generate the necessary masks with the more precise step-and-repeat camera methods. Typically, with these masks, fabrication capabilities at Georgia Tech would extend to approximately 0.4 μm. This limit is not only imposed by the camera techniques of the mask making but also by the wavelength of the UV light which our mask aligners use. The 300 nm UV radiation used in the photolithographic techniques limits the tightness of geometries attainable due to the large diffraction effects caused when the slit size and wavelength of incident light are of similiar lengths. In addition, reflection of the exposing light off the substrate tends to broaden the resulting resist patterns. These internal reflections can be corrected for in the masks to produce patterns of the desired size. This reflection can also be used to narrow the resultant geometries in positive photoresist techniques. To achieve the geometries that antennas for the infrared demand and especially the small geometries that may be dictated by the power converting devices, higher resolution techniques will be needed.

Two techniques which provide higher resolution to the fabrication process are electron beam and x-ray lithographic methods. Figure 24 illustrates the range these procedures provide [40]. The practical ranges have improved since the 1980 date of the figure in all but UV contact lithography which is restricted due to wavelength. The small wavelength of x-rays and electron beam techniques allow superfine resolution, and removes problems due to diffraction but does both at a higher price.

The electron-beam direct-write lithography uses the electron beam to define the photoresist pattern rather than employing a mask. This process is impractical for a large repetitive array of antennas for it is too time consuming. E-

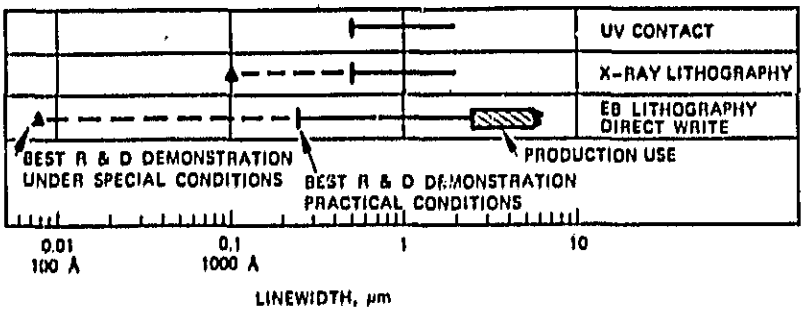

Figure 24. Limitations of various microfabrication Techniques [44].

beam exposure of the photoresist using a mask to define geometries is also impractical because the narrowness of the E-beam would require lengthy scanning times to cover the area to be developed. However, the E-beam direct write system could be used to generate a superior quality mask containing a high density of designs. With this mask used in conjunction with an x-ray source, a large highly resolved array could be generated. Available photoresist sensitive to x-rays, such as PMMA, allows 0.1 μm geometries to be produced. In addition, masks which have low attenuation of x-rays by the mask substrate (Si, Be, Si_3N_4, mylar) and high attenuation by the opaque layer (gold) have been made which meet or exceed our requirements [45].

For antennas of large size, the upper limit of the fly's eye camera is slightly larger than the 228 GHz antennas. This limit is due to the invariant spacing between adjacent patterns. If larger antennas are ever needed, standard photographic techniques can yield the desired masks.

VIII. Testing of Antennas

Fabrication of the rectenna array at 10.6 μm will require significant developement of existing technologies. Even if the system is developed for longer wavelengths where the microfabrication is not as difficult, the rectifying diodes for these frequencies will be a significant advance in the semiconductor technology. Therefore, a logical multi-phase program must be followed to achieve the eventual goal of the rectenna arrays/satellite power conversion system.

Phased programs for both the physical size of the rectenna elements and the detection/rectification device must be implemented. If the eventual goal is to produce power conversion capabilities at 10.6 μm, a three phase program, with an order of magnitude reduction in the physical size of the array elements at each step, seems to be a logical progression to follow. In this approach, the antenna and

detection/rectification technology is first developed for 1 mm wavelength radiation where the microfabrication procedure is not as demanding. When significant progress on the rectenna elements has been completed work on rectenna arrays for 100 μm radiation can begin. Likewise, when the major "bugs" are corrected at this intermediate size, the final step to 10.6 μm radiation can be taken.

The development of the detector/rectification element should also be a phased program. The first step in this effort is to produce a simple detection element to measure the antenna performance. Bismuth bolometers have already been shown to be successful for this task [40].

The next phase in this approach is to produce rectification of the incoming radiation with a very fast diode. Heiblum et.al. [43] have pioneered an edge MOM diode capable of detecting radiation into the optical region. This technology should be suitable to perform the first phase of the rectification development.

The second step in this process is to fabricate a bias-free diode with either dissimilar metals or semiconductor materials. This is a critical step if the rectenna arrays are to become operational. The final step will be to extend the diode technique to full wave rectification. This phase will yield a two-fold gain in the converted power.

Various testing procedures have been described in the literature [29]. At Georgia Tech, test procedures have been employed at 229 GHz for measurement of antenna parameters. These techiques are, in turn, appropriate for use at 10.6 μm.

Testing of the antennas at 229 GHz has shown their angular dependence to the field polarization and some frequency dependence. The inability to focus the radiation to a spot on the order of one wavelength has shown that the pad modification which was incorporated couples to an appreciable amount with the radiation. In addition, bonding wires and/or the fields

generate by the bias current interact with the source output and affect the level of coupled signal. The effect the wires had was lessened when the wires were tied-back and thereby, did not cross over the antenna's arms. Initially, the bonding pads were large due to constraints in our bonding equipment and expertise. New equipment that will be available plus the sharpening of techniques will allow for smaller bonding pads to be used. The next generation pads will be circular so as to avoid coupling.

The test facility for 229 GHz is shown in Figure 25. A cw Extended Interaction Oscillator (EIO) is employed as the radiation source. The EIO is capable of producing 2 watts of power. The EIO power supply is shown at the left of the figure, and at the right are signal generator for producing frequency-markers, spectrum analyzer for observation of beat frequency between multiplied frequency marker and the EIO, and a PAR Lock-in Amplifier for observation of the signal.

Figure 26 shows a closer view of the experimental apparatus. The signal from the EIO is propagated by a horn-lens configuration to the array of antenna/bolometers, which are mounted on a Burleigh Inchworm system. This arrangement allows an x-y scan of the arrays with a resolution on the order of one micron. The Inchworm system is mounted on a rotary table for determination of angular characteristics of the antennas. The signal is chopped for observations with the lock-in amplifier. The techniques employed here are independent of the observing wavelength.

IX. CONCLUSIONS AND RECOMMENDATIONS

A discussion has been presented of techniques for energy transfer and power conversion at millimeter and infrared wavelengths. Sources for power transfer exist at wavelengths from microwaves through the infrared, and the antenna/converter techniques, which are being investigated and are discussed in

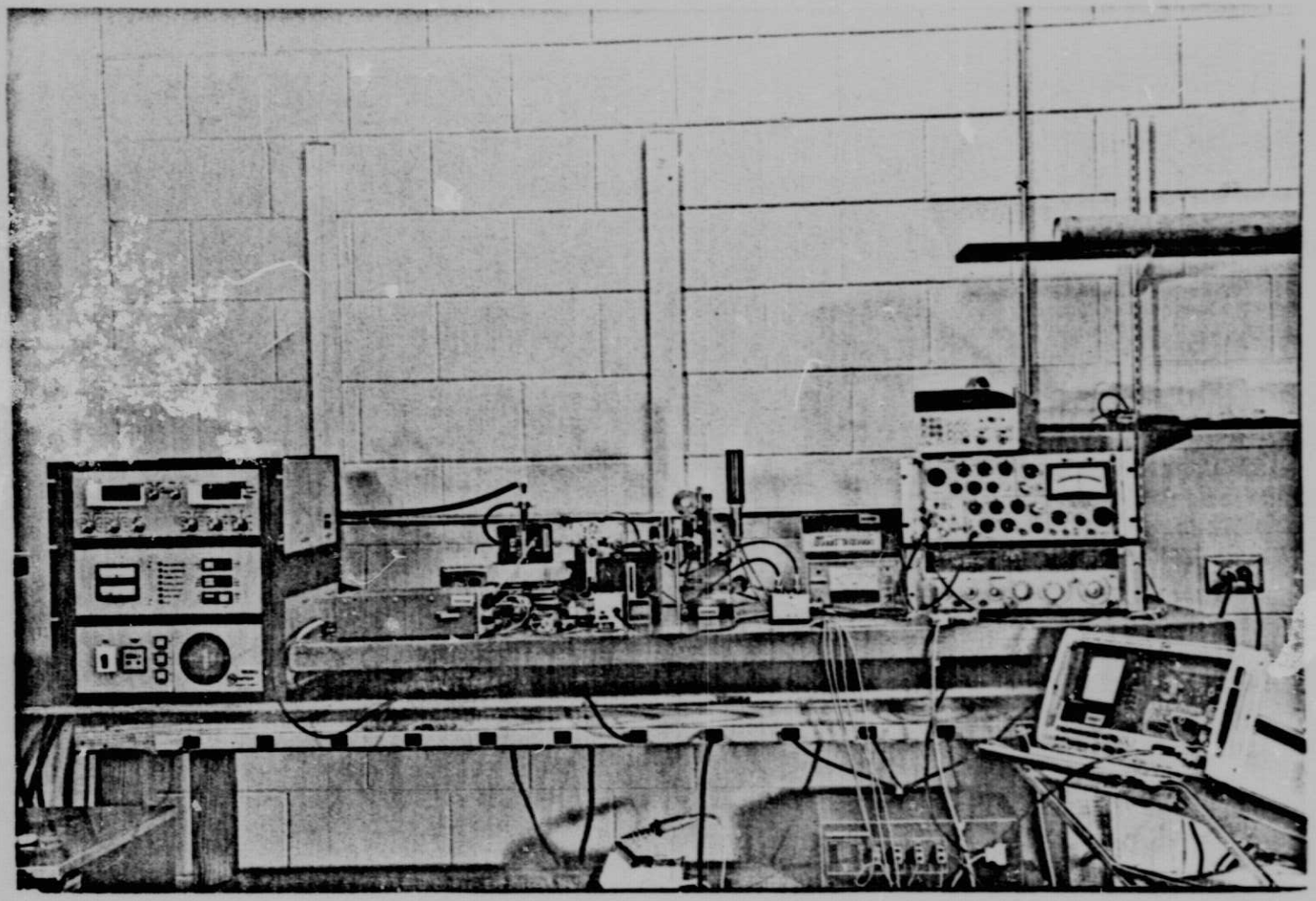

Figure 25. Antenna Testing Set-up at 229 GHz.

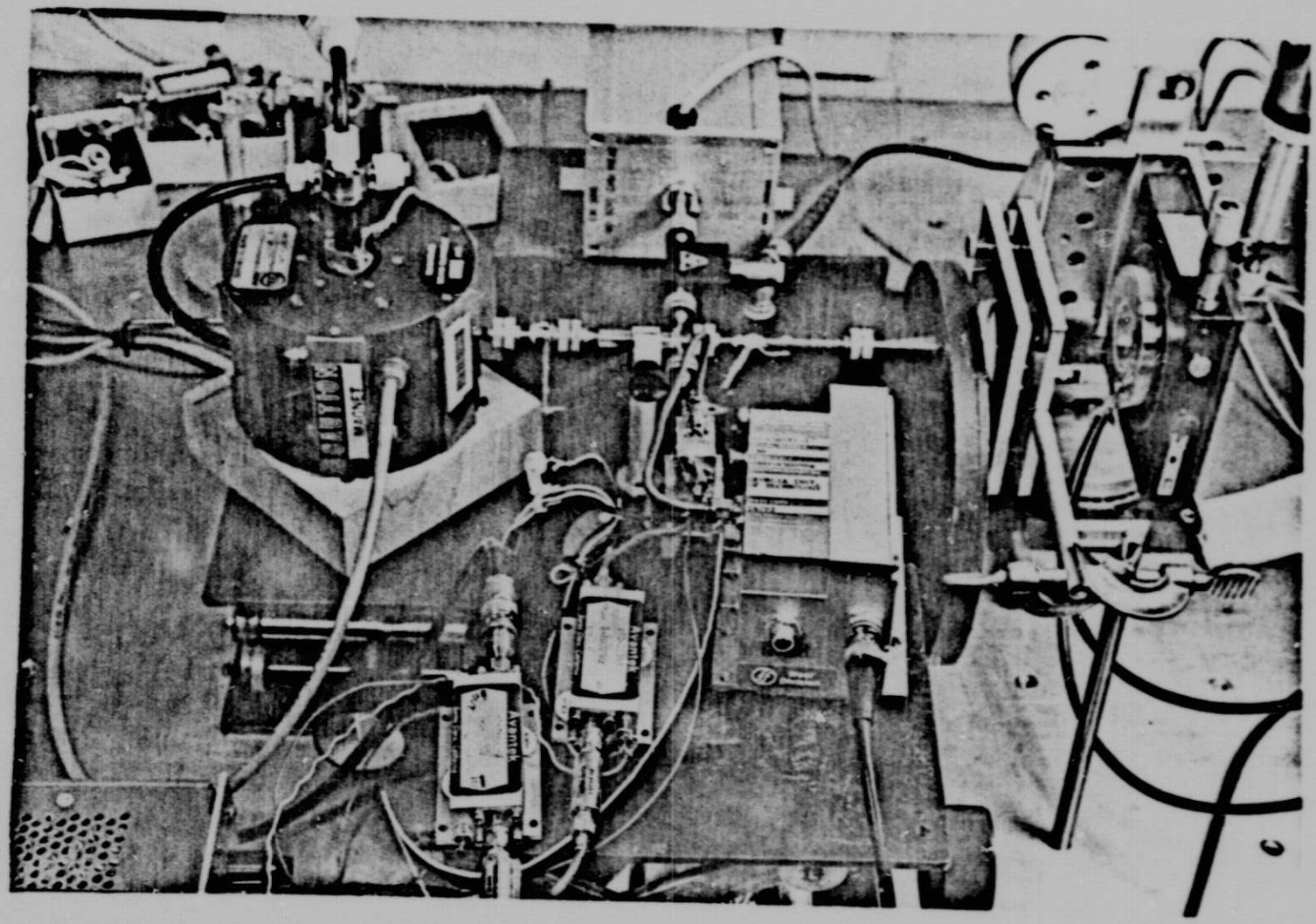

Figure 26. Detail of Antenna Testing Set-up at 229 GHz.

this report, are applicable for wavelengths into the infrared. Calculations [1] show that the earth's radiation should be capable of providing sufficient power density at satellite altitudes for operation of the vehicle systems. This radiation in the 8-12 μm region provides further reason for developing antennas and power converters at CO_2 laser wavelengths in the 10 μm region.

Investigations performed at Georgia Tech on miniature antennas have concentrated on half-dipole T-shaped antennas, but recent investigations [29] have shown different forms of antennas for the applications of interest here. A bow-tie antenna, of use over a broader bandwidth than the T-type antenna, may be more easily fabricated for the shorter wavelength applications. For propagation of coherent signals, either the CO_2 laser or longer wavelength sources can be employed. For operation at millimeter through submillimeter wavelengths, power transmission would have to be performed above the atmosphere or at high altitudes within the atmosphere. For power density delivered to a satellite antenna array, several considerations must be taken into account. Figure 27 [46] is an energy beaming nomograph showing the relations between wavelength, type and number of source, aperture, beamwidth, range, power of source, spot size at the array and power density delivered. This provides a convenient means of estimating the characteristics of a power transfer system.

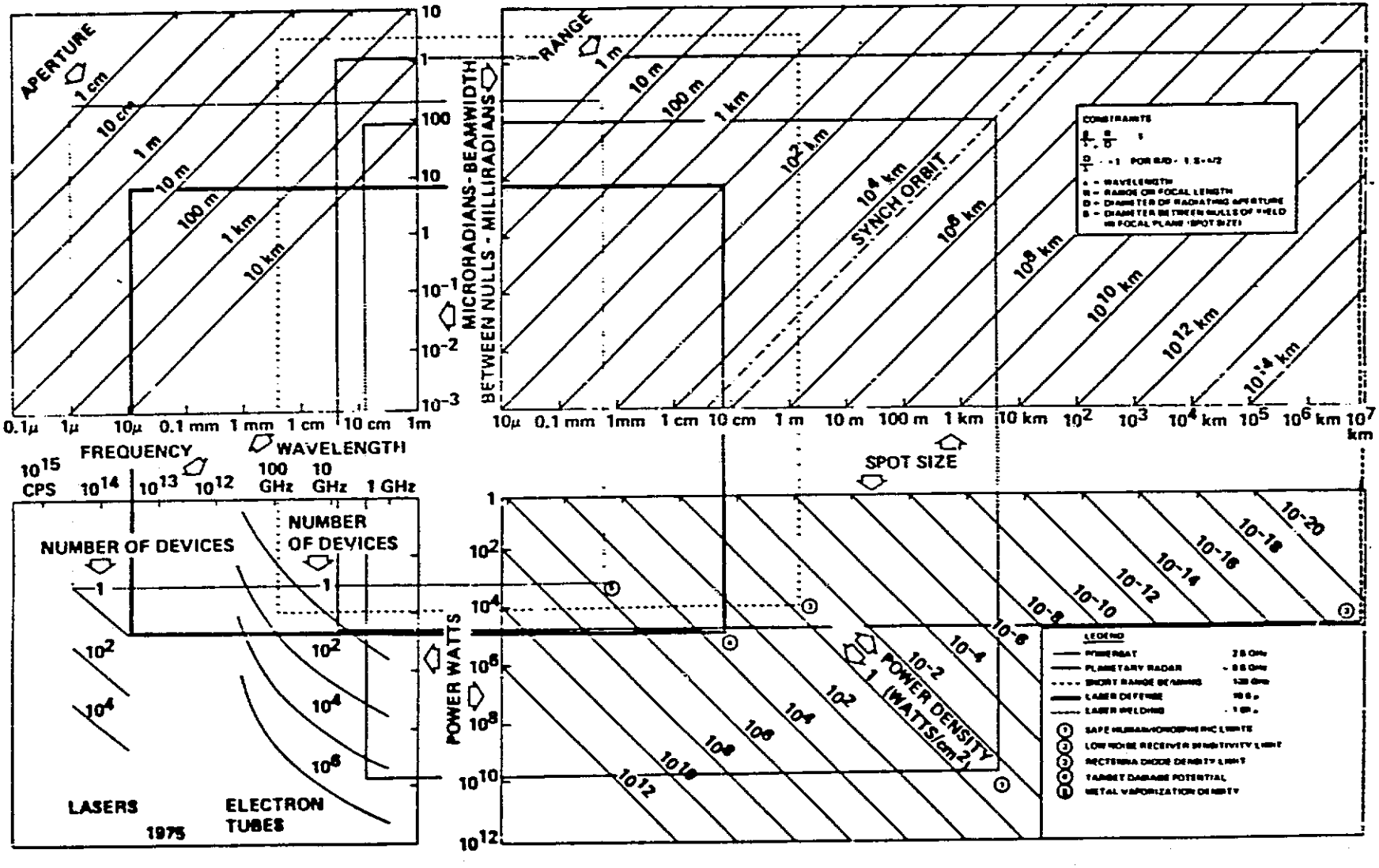

Figure 27. Energy Beaming Nomograph. [46]

REFERENCES

1. J. J. Gallagher, C. J. Summers and D. P. Campbell, "Infrared Technology for Satellite Power Conversion," NASA Research Grant No. NAG3-282, Semi-Annual Report, January, 1983.
2. M. Mizushima, "Transparency of Earth's Atmosphere in the Frequency Region Below 1 THz", Intern. Journ. Infrared and Millimeter Waves, 3, #6, pp. 889-895 (1982)
3. R. W. McMillan, "Near Millimeter Wave Sources of Radiation," Proc. IEEE (to be published, 1985)
4. V.A. Flyagin, A.V. Gapanov, M.I. Petelin, and V.K. Yulpatov, "The Gyrotron," IEEE Trans. Microwave Theory Tech., MTT-25, 6, June 1977, pp 514-521
5. J.L. Hirshfield, "Gyrotrons," Chapter 1, Infrared and Millimeter Waves, Vol. 1., K.J. Button, ed., Academic Press, New York, 1979
6. P. Sprangle and T. Coffey, "New Sources of High-Power Coherent Radiation," Physics Today, pp 44-51 (March, 1984)
7. Y. Carmel, K.R. Chu, M. Read, A.K. Ganguly, D. Dialetis, R. Seeley, J.S. Levine, V.L. Granatstein, Phys. Rev. Lett. 50, 112 (1983)
8. H. Jory, R. Bier, S. Evans, K. Felch, L. Fox, H. Huey, J. Shively and S. Spang, "First 200 kW cw Operation of a 60 GHz Gyrotron," International Electron Devices Meeting, Washington, D.C., Dec., 1983, Paper 11.2, pp 267-270
9. J. Eckstein, D. Latshaw, and D. Stone, "Performance of a High Power 95 GHz Gyro-TWT Amplifier," 1984 Microwave Power Tube Conference, Paper 15.1, Monterey, California, May 1984.
10. M.R. Read, K.R. Chu and A.J. Dudas, "Experimental Examination of the Enhancement of Gyrotron Efficiencies by Use of Profiled Magnetic Fields," IEEE Trans. Microwave Theory & Techniques, MTT-30, #1, pp 42-46 (Jan., 1982)

11. J.F. Shively, P. Ferguson, H.R. Jory, J. Moran and R.S. Symons, "Recent Advances in Gyrotrons," 1980 IEEE MTT-S International Microwave Symposium Digest, pp 99-101 (June, 1980)
12. H. Jory, R. Bier, K. Felch, L. Fox, H. Huey, N. Lopez and S. Spang, "Progress in cw Gyrotron Oscillators," 1984 Microwave Power Tube Conference, Paper 13.1, Monterey, California, May 1984
13. W.W. Destler, R.L. Weiler and C.D. Striffler, "High Power Microwave Generation from a Rotating E Layer in a Magnetron-type Waveguide," Appl. Phys. Lett. 38, pp 570-572 (1981)
14. Y.Y. Lau and L.R. Barnett, "A Low Magnetic Field Gyrotron-Gyro-magnetron," Int. Journ. Electronics 53, #6, pp 693-698 (1982)
15. P. Ferguson, W. DeHope, V. Matranga, J. Sandoval, M. Schmitt, J. Tancredi and C. Thornington, "A High-Efficiency High-Power 100 GHz Gyrotron," Paper 13.2, 1984 Microwave Power Tube Conference, Monterey, California, May, 1984
16. D. A. G. Deacon, L. R. Elias et al, Phys. Rev. Lett. 38, 892 (1977)
17. A. Renieri, Theory and Development of Infrared Free-Electron Lasers, pp. 174-182, Proceedings of the Third International Conference on Infrared Physics, Switzerland, July 23-27, 1984
18. K. Kuwabara, H. Sugawara, T. Shirakura, K. Sasaki, and S. Takemori, "Gas Laser Device," U.S. Patent 4 331 939, May 25, 1982
19. A. Sona, "Research Programs In Italy on High Power Lasers and Their Application to Metalworking," presented at the International Conference of Welding Research in the 1980's, Oct. 27-29, 1980, (Osaka, Japan), NTIS #N81-24438/6.

20. T. Okada and T. Takemoto, "Engineering Design of a Fast Axial Flow 6kW Laser," in Advanced Welding Technology in 1981, Proc. of the Japan-UK-USA Joint Seminar, (Japan), pp. 74-83, Japan: Japan Welding Scoiety, 1981.
21. J. D. Russell and R. C. Crafer, "The Development of a 6kW Laser," in Advanced Welding Technology-in 1981, Proc. of the Japan-UK-USA Joint Seminar, (Japan), pp. 54-73, Japan: Japan Welding Society, 1981.
22. M. W. Sasnett, "Comparing Industrial CO_2 Lasers," Lasers and Applications, vol. 3, no. 9, pp. 85-90, 1984.

24. W. B. Tiffany, R. Targ and J. D. Foster, "Kilowatt CO_2 Gas - Transport Laser," Appl. Phys. Lett., vol. 15, pp. 91-93, 1969
25. T. J. Bridges and C. K. N. Patel, "High-power Brewster Window Laser at 10.6 microns," Appl. Phys. Lett., vol. 7, pp. 244-245, 1965
26. P. K. Cheo, "Effects of Gas Flow on Gain of 10.6 micron CO_2 Laser Amplifiers," IEEE J. Quant. Elect., vol. QE-3, pp. 683-689, 1967
27. K. Gurs, "Research and Development in the Field of High Power Laser Technology at Battelle," in Proc. of the SPIE, vol. 455, pp. 10-16, 1984.
28. R. E. Beverly III, "Kinetic Modeling of a Fast Axial Flow Laser," Optical and Quantum Electronics, vol. 14, pp. 25-40, 1982
29. D. B. Rutledge, D. P. Neikirk, and D. P. Kasiligam, in "Infrared and Millimeter Waves," vol. 10 (K. J. Buton, ed.) pp. 1-90, 1983
30. S. Ramo, J. R. Whinnery and T. Van Duzer, "Fields and Waves in Communication Electronics", Wiley, New York, 1965
31. D. B. Rutledge, "Submillimeter Integrated Circuit Antennas and Detectors," Ph.D. Thesis, University of California, Berkeley, California, 1980

32. C. R. Brewitt-Taylor, D. J. Gunton, and H. D. Rees, Electon Lett., Vol. 17, pp. 729-731, 1981
33. H. Jasik, "Antenna Engineering Handbook," McGraw-Hill, New York, 1961
34. J. Galejs, IRE Trans. Antennas Propagation, Vol 10, pp 435-443, 1962
35. A. Banois, "Dipole Radiation in the Presence of a Conducting Half-Space," Perganom, Oxford, England, 1966
36. R. W. King, and G. S. Smith, "Antennas in Matter," MIT Press, Cambridge, Massachusetts
37. P. T. Parrish, et. al. SPIE Proc. vol. 337, Millimeter Wave Technology, May 6-7, 1982
38. D. B. Rutledge and M. S. Muha, IEEE Trans. Antenna Propag., vol. AP-30, pp. 535-540, 1982
39. D. P. Neikerk, P. P. Tong, D. B. Rutledge, H. Park, and P. E. Young, Appl. Phys. Lett., vol. 41, pp. 329-331, 1982
40. D. P. Campbell, J. J. Gallagher, and M. A. Gouker, "5th Interim Status Report on Infrared Technology for Satellite Power Conversion", NASA Research Grant No. NAG3-202, in preparation, 1984
41. S.M. Sze, Physics of Semiconductor Devices, (John Wiley - Sons, New York, 1981) p. 566.
42. J. Simmons, Journ. Appl. Phys. 34, 2581, (1963)
43. M. Heiblum, S.Y. Wang, J.R. Whinnery and T.K. Gustafson, "Characteristics of Integrated MOM Junctions at DC and at Optical Frequencies," IEEE J. Quantum Electron., QE-14, 159 (1978).
44. G. R. Brewer, "In "Electron-Beam Technology in Microelectronic Fabrication," (G.R. Brewer, ed.), Academic Press, New York, 1980
45. J. Trotel and B. Fay, In "Electron-Beam Technology in Microelectronic Fabrication," (G. R. Brewer, ed), Academic Press, New York.

46. E. J. Nalos, "New Developments in Electromagnetic Energy Beaming," Proc. IEEE, 66, 276, (1978)